



# Surface plasmon resonance technology: Recent advances, applications and experimental cases



Davide Capelli, Viviana Scognamiglio, Roberta Montanari\*

*Institute of Crystallography, National Research Council, Department of Chemical Sciences and Materials Technologies, Via Salaria km 29.300, 00015, Monterotondo, Rome, Italy*

## ARTICLE INFO

### Article history:

Received 13 December 2022

Received in revised form

23 March 2023

Accepted 26 April 2023

Available online 3 May 2023

### Keywords:

Surface plasmon resonance

Biosensor

Surface plasmons

Optical devices

Commercial systems

Sensor chips

## ABSTRACT

In the modern era of advanced technologies, rapid and accurate analyses are needed, both for scientific research and for industrial applications. For this reason, the Surface Plasmon Resonance (SPR) technology emerged as very successful particularly in the last ten years, being capable of measuring interactions in real time with high sensitivity and without the need for labels. Thanks to these characteristics, SPR has gained great popularity and represents a viable choice for many applications, from life sciences to pharmaceuticals, agrifood and environmental monitoring of harmful substances. Herein, we examine the recent advances in the development of SPR technology to provide an excursus on the various types of instrumentation available on the market, discuss their advantages and their limitations as well as future trends, and to analyze particular case studies addressed by SPR technology.

© 2023 Elsevier B.V. All rights reserved.

## 1. Introduction

The phenomenon of Surface Plasmon Resonance (SPR) gives rise to a spectroscopic method that allows for real-time monitoring of the interactions between a free analyte in solution and a biomolecular recognition element immobilized on the sensor surface to detect and capture a target analyte of interest [1,2]. Moreover, thanks to the lack of susceptibility to the matrix effect, SPR has the advantage of using minimal amounts of real and unlabeled samples making sample pretreatment unnecessary [3]. This results in a highly sensitive, very versatile and capable technology, which has given rise to thousands of research articles [4–6], in-depth reviews [7,8] and books [9–11] over the past decades. Indeed, a "Surface Plasmon Resonance" search on the ISI Web of Science yields over 63,000 publications (April 2022), with the number of publications doubling in 2020 when compared to 2010.

In detail, SPR is a physical process that can occur when plane-polarized light hits a thin semitransparent metal film (usually gold or silver) that is deposited on the base of a total internal

reflection prism with high refractive index (RI). At a certain critical angle of incidence ( $\theta$ ), the incident light photons are absorbed in the metal surface and the energy is transferred to the electrons, which convert into surface plasmons (SPs) [12,13] (Fig. 1A). At this point, all the incoming light reflects within the circular prism, resulting in a total internal reflection. This allows for quantitatively recording the adsorption of biomaterials at the interface, because SPs excited along the metal-dielectric interface lead to a dramatic reduction of the reflected beam intensity and to the formation of reflection conditions [14]. Such conditions are very sensitive to any changes taking place in the close proximity to the metal-dielectric interface, such as the adsorption of molecules onto the metal surface and the formation of the layers of molecules. This allows for the detection of the binding of very low amounts of material thanks to the very high sensitivity towards small changes in the refractive index near the surface [15]. Indeed, the affinity interactions cause a refractive index variation, which is measured as a change in resonance angle and can be detected by providing analytical signals that are proportional to the change in mass concentration upon the sensing surface (Fig. 1B). The downside is that any outer changes such as solvent composition, pH, ionic strength and temperature and other causes of instrumental drift can negatively affect the signal detection [16,17].

SPs were first discovered between 1902 and 1912 by R.W. Wood

\* Corresponding author. Institute of Crystallography, National Research Council, Department of Chemical Sciences and Materials Technologies, Via Salaria km 29.300, 00015, Monterotondo Scalo, Rome, Italy.

E-mail address: [roberta.montanari@ic.cnr.it](mailto:roberta.montanari@ic.cnr.it) (R. Montanari).

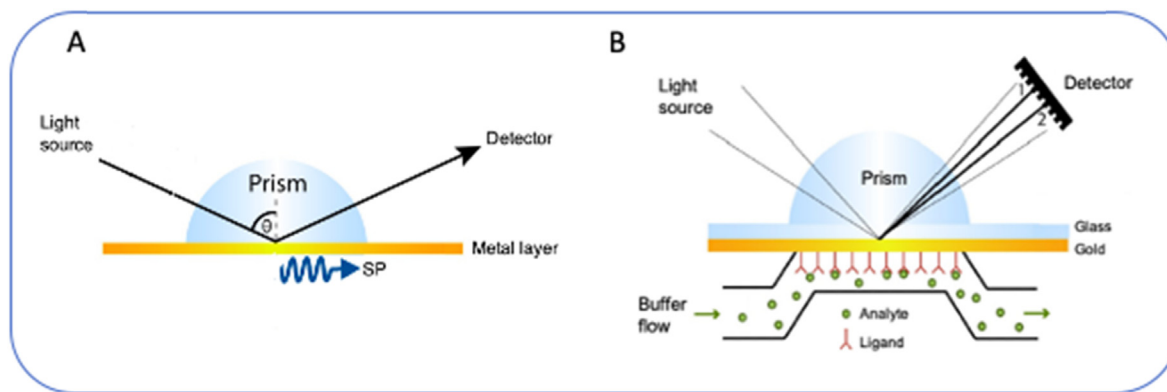


**Fig. 1.** Representation of the Kretschmann-Raether configuration used for optical excitation of SPs. (A) At a certain angle  $\theta$ , the energy is transferred from the light into the surface plasmon and surface plasmon resonance occurs. (B) As molecules bind, the refractive index close to the surface changes causing a shift in the angle ( $1 \rightarrow 2$ ). The change in angle is proportional to the mass of bound material.

at Johns Hopkins University (Baltimore, USA), who noticed a pattern of unusual dark and light bands in the spectrum of diffracted light on a metal diffraction grating [18,19]. In 1941 Fano concluded that these anomalies were associated with surface (lattice) waves supported by the network [20]. Later, in 1958, Thurbadar observed a sharp drop in reflectivity when illuminating thin metallic films on a substrate, but did not link this effect to SPs [21]. It was in 1968 that Otto demonstrated that the decline in reflectivity in the attenuated total reflection method is due to the excitation of the SPs [22].

In the same year, Kretschmann and Raether observed SPs excitation in another configuration of the total attenuated reflection method (Fig. 1A) [23]. The pioneering studies of Otto, Kretschmann and Raether introduced SPs into modern optics which, in the late 1970s, were applied to the study of biological and chemical interactions. In 1980 Pharmacia became interested in the SPR technique and in 1984 founded the company Pharmacia Biosensor AB to develop, manufacture and market a functional SPR machine. Since then, SPR sensors have made enormous progress in terms of both technological development and applications. Generally, the basic components of a SPR sensor are: *i*) an optical light source, which is often a near-infrared, high-efficiency light-emitting diode (LED); *ii*) an optical coupling component (prism, grating, waveguide, or optical fiber); *iii*) the sensor chip, which is a glass layer coupled to a planar metal layer upon which the molecule of interest is immobilized; *iv*) the detection system, which is commonly a charge-coupled device (CCD) that uses a linear array of light-sensitive diodes or pixels to cover the range of incident light angles; *v*) the fluid handling system, which provides a consistent stream of buffer flowing across the sensor chip to maintain a controlled environment (Fig. 2A).

As fluidics and non-specific responses strongly influence the accuracy of an SPR sensor based on the Kretschmann-Raether setup, SPR sensing devices are required to distinguish specific sensor response (due to the binding of the analyte with the ligand immobilized on the sensor surface) from the non-specific response (refractive index changes caused by temperature and sample composition variations and adsorption of non-target molecules to the surface) [24]. In recent years, multichannel SPR devices including sensing channels with ligands for the detection of specific analytes and reference channels responding only to non-specific binding have been manufactured (Fig. 2B).

Given the large number of applications of SPR technology (Fig. 3), the development of new multi-channel multi-parameter SPR sensors with high integration density, high productivity and

simultaneous measurement of multiple sites has become the subject of increasing attention [25,26].

Herein, we introduce SPR basic principles and technology to the reader and we provide an overview and comparison of the current SPR platforms available on the market, with a wide summary of the related sensor chips and their primary utilization. Moreover, in the present review we analyze potential applications of SPR in various fields through the critical discussion of different case studies and we examine the recent advances in the development of SPR sensing technology.

## 2. Commercially available SPR instruments

Because of the large range of applications of the SPR technique, more companies are currently in the market with many instruments enabling distinct performances based on differences regarding their optical system, their degree of development, and their automation [27]. Thus, the choice of an SPR system depends on a number of factors including throughput and samples scope of the research, as well as flexibility, cost and ease-of-use of the platform to be purchased.

Usually, if a high-throughput workflow is desired, a platform enabling multi-channel analysis will represent the best solution, whereas two-channel instruments are typically sufficient for academic labs and relatively low throughput needs. Besides this general consideration, some other common specifications of an SPR system must be considered to better meet a specific experimental purpose: *i*) the sample injection volume; *ii*) the baseline noise to ensure the best signal-to-noise ratio; *iii*) the baseline drift for good data fitting; *iv*) the temperature range, particularly for thermodynamic measurements; *v*) the flow rate range, that must be faster for more accurate kinetics.

This paragraph provides an overview of some of the SPR instruments currently available on the market with a brief description of the main features and characteristics. For more comprehensive details about the described instrumentations see Table 1 or visit the vendors' websites.

Since SPR was first introduced in the early 1990s, Biacore™ has represented for many years the pivotal company for the manufacture of instrumentation designed to measure biomolecular interactions and its products are still considered the most reliable on the market. Among them, Biacore™ S200 is currently the most sensitive SPR-based sensor, facilitating work with low-level responsive targets such as low-molecular-weight (LMW) molecules in the LMW/fragment drug discovery process. Recently,

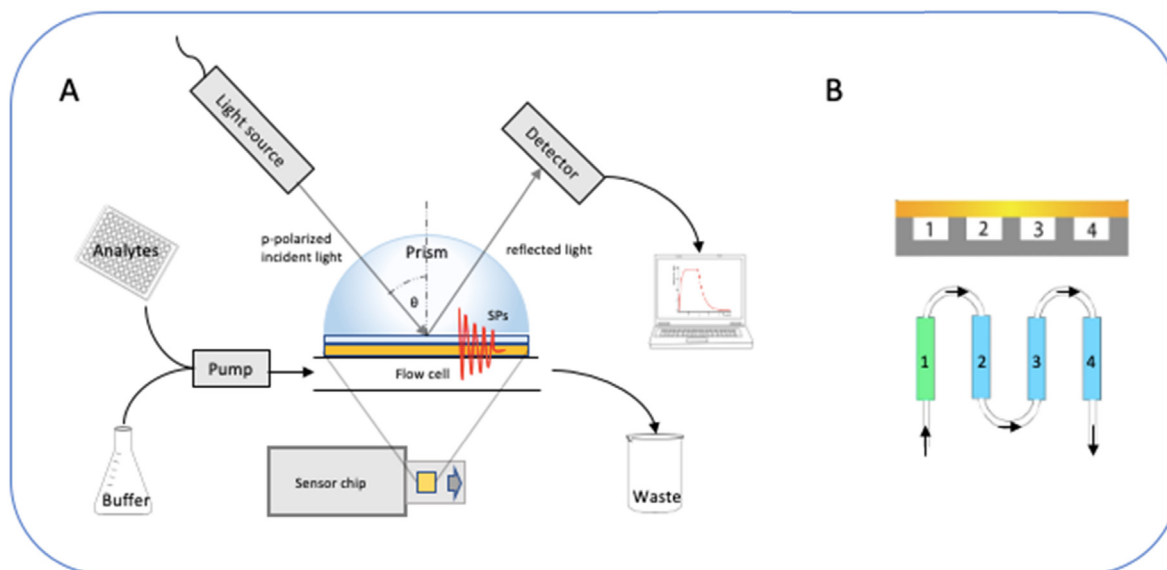


**Fig. 2.** (A) Block scheme of the main components of a prism-based SPR instrument. (B) Magnification (top) and schematic representation (bottom) of serial flow cells showing the reference channel (green) and the sensing channels (cyan).

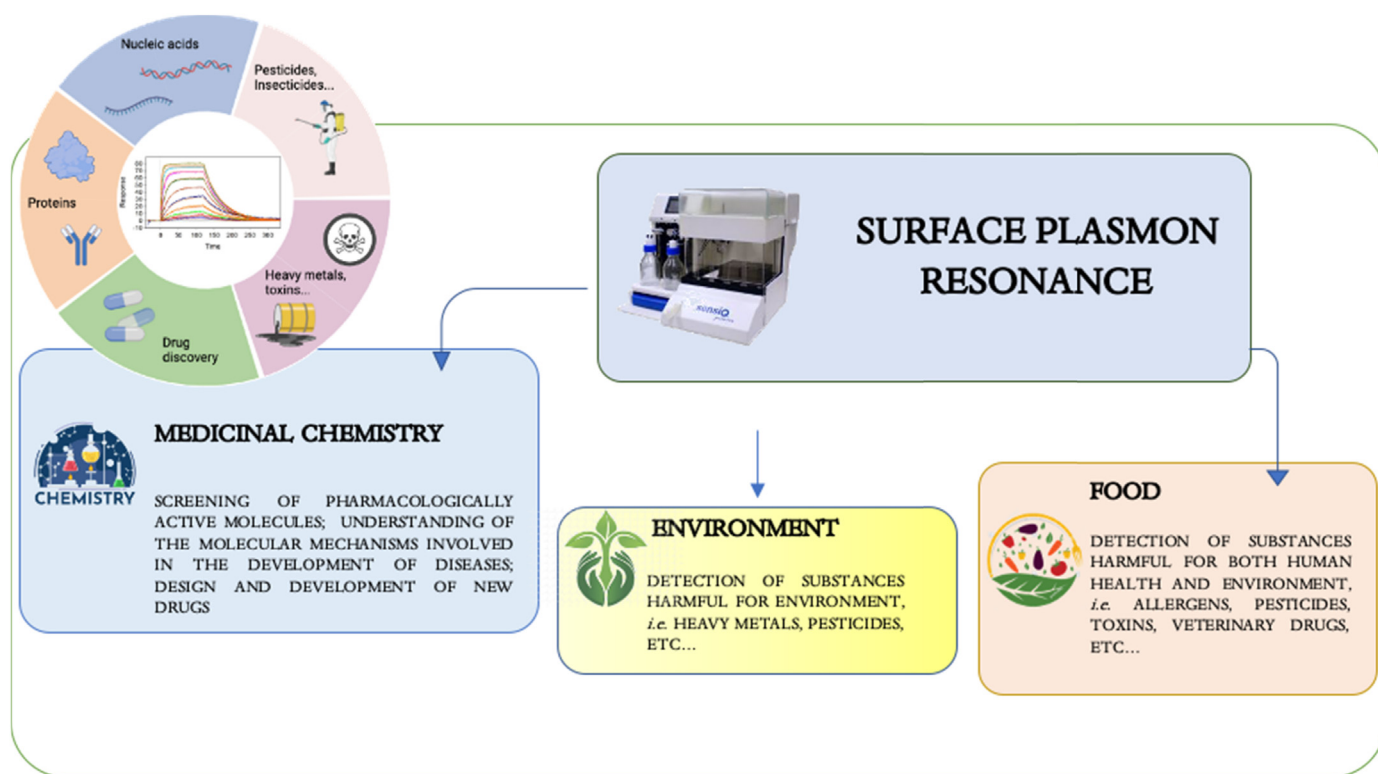


**Fig. 3.** Schematic representation of different applications of Surface Plasmon Resonance.

Biacore™ 8K + has been presented as a high-throughput and high-sensitivity eight needle SPR system that delivers binding data of outstanding quality in screening, characterization and quality control, with a maximized capacity of up to 4608 samples [28].

Similarly, Bruker recently presented the Sierra SPR®-24/32 Pro, which has the features expected from a high-throughput system, including 8 flow cells with either 32 or 24 individually addressable sensors and high-sensitivity SPR + imaging detection [29].

However, during the last decade, many companies have expanded their commercial offer on the market by introducing new platforms, which differ in the way of using the technology and design of bringing the interactants in contact with each other. Thus, besides the canonical prism-coupled total reflection systems, several different configurations of SPR devices have been developed, such as those using grating, fiber and waveguide-coupling SPR sensing mechanisms [15,30].

**Table 1**

Overview of the SPR instrument in commerce with main features and specifications as described on the vendors' website.










INSTRUMENT	MAIN FEATURES	SPECIFICATIONS	PICTURE
<b>Biacore™ S200</b>	High sensitivity High-throughput LMW/fragment drug discovery ABA injection type for competition assay	Application: kinetics/affinity characterization, kinetics/affinity screening, single-cycle kinetics, LMW interaction analysis, fragment screening, epitope mapping, thermodynamics Analysis temperature: 4 °C–45 °C Baseline drift: <0.3 RU/min Baseline noise: <0.015 RU (RMS) Capacity: 1 × 96- or 384-well microplate and up to 33 reagent vials or 78 vials for samples and reagents Flow rate: 1–100 µl/min Injection volume: 2–350 µl Molecular Weight Limit: No lower limit Number of flow cells: 4 Sample type: Small-molecule drug candidates to high-molecular weight proteins (DNA, RNA, polysaccharides, lipids, cells, and viruses) Sample recovery: yes	
<b>Sierra SPR®-24/32 Pro</b>	High sensitivity High-throughput LMW/fragment drug discovery Hydrodynamic Isolation (HI) microfluidic technology	Application: high-throughput applications such as epitope characterization and antibody, LMW/fragment screening Analysis temperature: 10 °C–37 °C Baseline drift: <0.15 RU/min Baseline noise: <0.02 RU (RMS) Capacity: 96-well (standard, medium or deep) or 384-well (standard or deep) microtiter plates and reagent rack with 24 × 0.8 ml vials, 40 ml or 2 × 19 ml troughs Flow rate: 5–100 µl/min Injection volume: 2–200 µl Molecular Weight Limit: No lower limit Number of flow cells: 8 Sample type: Small-molecule drug candidates to crude samples, serums and supernatants, as well as membrane preparations and vesicles Sample recovery: ND	
<b>Sartorius Octet® SF3</b>	High sensitivity High-throughput LMW/fragment drug discovery OneStep® and NeXtStep™ gradient injection technology	Application: kinetics/affinity characterization, high-throughput applications (epitope characterization and LMW/fragment screening) and competition assay Analysis temperature: 4–40 °C (max 15° below ambient) Baseline drift: <0.3 RU/min Baseline noise: <0.025 RU (RMS) Capacity: 2x sample racks (96-vial, deep well and PCR formats, 384-well microplates, custom high volume) plus 2x reagent racks Flow rate: 0.1–200 µl/min Injection volume: 2–700 µl Molecular Weight Limit: No lower limit Number of flow cells: 3 Sample type: small and large molecules Sample recovery: yes	
<b>Creoptix® WAVEdelta</b>	High sensitivity High-throughput LMW/fragment drug discovery Grating-Coupled Interferometry (GCI) technology No clog microfluidic	Applications: kinetics/affinity characterization, LMW interaction analysis Analysis temperature: 4–45 °C (max 20 °C below ambient) Baseline drift: <0.3 RU/min Baseline noise: <0.01 RU (RMS) Capacity: 2x microtiter plates (96 or 384 well, standard or deep well) or vial racks (48 positions of 1.5 ml) Flow rate: 1–400 µl/min Injection volume: <450 µl, 100 µl typical Molecular Weight Limit: No lower limit Number of flow cells: 4 Sample type: small and large molecules, crude samples, blood, harsh chemicals and particles up to 1000 nm Sample recovery: yes	
<b>2SPR-Plus system</b>	High sensitivity LMW/fragment drug discovery Upstream/downstream connection with other techniques (LC or MS)	Applications: kinetics/affinity characterization, concentrations, thermodynamics Baseline drift: <0.1 RU/min Baseline noise: 0.05 RU (RMS) Capacity: 12 to 768 samples Analysis temperature: 4 °C–70 °C (max 10 °C below ambient) Flow rate: 0.1–3,000 µl/min Injection volume: 1–4,500 µl (depends on installed loop volume) Molecular Weight Limit: <100 Da Number of flow cells: 2 Sample type: small and large molecules; crude samples, serum, cell lysates, liposomes Sample recovery: ND	
<b>White FOX</b>	Easy-to-use benchtop device No fluids: no clogging, no cleaning Cost-effective User-friendly software	Applications: kinetics/affinity characterization, quantification of proteins and antibodies, sandwich assays Baseline drift: ND Baseline noise: ND Capacity: 96 well plate; 96 probes Analysis temperature: ambient to 42 °C	

Table 1 (continued)

INSTRUMENT	MAIN FEATURES	SPECIFICATIONS	PICTURE
<b>Affinité P4SPR</b>	Portability USB powered User-friendly Cost-effective	Flow rate: ND Injection volume: 140 µl/well; non-destructive testing Molecular Weight Limit: ND Number of flow cells: Sample type: proteins, antibodies, nanobodies, complex particles, vesicles, viruses, blood Sample recovery: yes Applications: kinetics/affinity characterization, quantitative measurements Size (W) x (L) x (H): 175 × 155 × 55 mm Weight: <1.3 kg Resolution: 1 RU Number of flow cells: 4 Sample type: small and large molecules; complex media such as serum, plasma, cell lysates, wastewater	
<b>H5 PhotonicSys'</b>	Portability Combination with other inspection equipment Friendly Graphical User Interface (GUI)	Applications: kinetics/affinity characterization, quantitative measurements Size (W) x (L) x (H): 216 × 76 × 51 mm or smaller Weight: <1 kg Resolution: <1 RU Number of flow cells: 2 or more upon request Sample type: small molecules and large bioentities (viruses, bacteria, cells)	
<b>Plasmetrix CORGI IIF SPR System</b>	Portability and modularity USB 3.1 powered Cost-effective For research & education	Applications: kinetics/affinity characterization, specificity, concentration, electrochemical Size (W) x (L) x (H): 80 × 150 × 40 mm Weight: ND Resolution: 1 RU Number of flow cells: 2 Sample type: proteins, antibodies, lipids, nanoparticles, peptides, viruses	

Although based on traditional SPR, the Sartorius Octet® SF3 system can characterize a wide range of interactions with high quality kinetics and affinity data for up to 768 samples in a single unattended assay [31]. The Octet® SF3 system incorporates the OneStep® injection technology, based on the well-established concept of Taylor dispersion injection [32], which allows the compound to diffuse into a moving stream of buffer to generate a concentration gradient during the injections. As such, a single analyte injection can be used to measure data accurately, providing better resolved kinetic traces and rapid affinity data directly from primary screens, significantly reducing the time and costs associated with secondary screening [33]. The Octet® SF3 system has a higher sensitivity and also incorporates NextStep™ gradient injection technology, which distributes two different analytes against each other in a crossed sigmoidal profile and can be used for determining competition mechanisms or inhibition concentration (IC<sub>50</sub>) in a single injection [34].

Malvern Panalytical newly introduced on the market the Creoptix® WAVEdelta, a novel optical biosensor platform for high sensitivity and real-time label-free binding kinetics. The WAVE system is based on the Grating-Coupled Interferometry (GCI) technology and can support a wide range of sample types and sizes thanks to the no-clog microfluidic cartridges, which allow high-sensitivity data analysis also from difficult crude samples [35].

In recent years, Xantec significantly expanded the potentiality of SPR with the 2SPR-Plus system [36], based on Reichter's 2-channel SPR platform [37], which combines SPR with other techniques such as Mass Spectrometry and preparative Liquid Chromatography, eliminating the limitations of all SPR platforms commercially available.

FOx Biosystems newly presented the White FOx instruments based on fiber optic SPR as sensor tool bioanalysis. In this robust, low-maintenance and easy-to-use device, the fiber-optic probe setup allows a fluidic-free dip-in protocol for the study of specific

biomolecule binding in complex samples including lysates, whole blood and large particles, avoiding clogging issues and routine cleaning [38].

Finally, many companies have developed small size devices that still retain high-performance and reliability features. For instance, the Affinité P4SPR is an accessible cost unique portable 4-channel instrument that delivers measuring and monitoring data of specific targets in complex media, giving also the possibility to combine with other analytical methods such as spectroscopy, chromatography and mass spectrometry [39]. Similarly, PhotonicSys' devices can be standalone or integrated into other systems comprising optical microscopes, fluorescence and Raman systems due to their miniaturized size [40]. Plasmetrix has also specialized in compact, portable and modular devices at affordable prices for research and education. The tiny CORGI IIF SPR System measures only 15 cm in length, packing a lot of options and add-on configurations keeping high versatility and great performances [41].

An overview of some of the SPR instruments currently available on the market with a description of the main features and characteristics is reported in Table 1.

### 3. SPR sensor chips

The sensor chip can be considered the core of an SPR biosensor and its surface chemistry has a great influence on the behavior of the SPR device and the quality of the data retrieved [42]. The variety of existing sensors and the different sensing schemes indicate that a plasmonic solution can be found for an array of biochemical and biomedical problems, from fundamental studies of protein-protein interaction to disease diagnosis through the detection of biomarkers at very low concentrations in complex biological samples [43]. Indeed, a wide range of applications has been developed for the use of SPR biosensors both in the biomedical field and in pharmaceutical research [44,45]. In addition, they have been

increasingly applied in the detection of chemical and biological species in important areas such as environmental monitoring, and food safety and security [7,44,46].

As depicted in Fig. 4A, the base of a sensor is a thin glass slide. A metallic layer (~50 nm), which can generate surface plasmon by coupling with a p-polarized beam of light, is deposited on one side of the slide and a very thin adhesion layer (~2 nm) of Chromium or Titanium is inserted between the glass and the plasmonic metal layer, thus improving the stability of the metal film [47].

Particularly for commercial sensor chips, gold still represents the best choice among plasmonic metals because it combines favorable SPR characteristics (*i.e.* low optical losses for SPs excitation) with long-term chemical stability under a wide range of conditions, including pH and moderate concentrations of many organic solvents [48,49]. Although the wide assortment of the different surface functionalization commercially available provides application-specific immobilization basis for all possible ligand–analyte combinations, unmodified gold sensors are also supplied from some vendors allowing the design and the creation of unique customized surfaces. Moreover, in the search for cost reduction possibility and higher sensitivity, the gold metal film can be replaced by other metals such as silver and copper, especially for disposable sensor applications. Silver-based SPR sensors show greater sensitivity and sharper reflectivity spectrum than those of gold film, along with an improved limit of detection (LOD) and

resolution. However, the poor chemical stability that results in oxidation and sulfuration restricts their application in this field. Nevertheless, in recent years more sensitive and stable silver-based SPR sensors have been improved and tested as a good alternative to the gold ones [50,51]. A still rarely explored alternative is the replacement of the gold film by a more affordable copper film, which has the highest electrical conductivity among the metals and exhibits almost identical optical properties, but it is still considered as a poor plasmonic material because of its notorious oxidation issues when subjected to air exposure. All of these considerations encouraged efforts to explore copper utilization in the plasmonic application looking forward to the possibility of the integration of such SP-sensing elements into electronic devices [52,53].

Since the metal layer is in most cases incompatible with biological species, the surface must be protected against the non-specific adsorption of proteins or other biological compounds. The pacification layer (~2 nm) should bond tightly to the gold layer and form a compact packaging, effectively shielding the metal layer. In general, the pacification layer - also referred to as Self-Assembling Monolayer (SAM) - has terminal functional groups that can be used for further modifications of the sensor surface. In this way, the most appropriate surface chemistry and density can be chosen among a wide range of possibilities and exploited for the study of the various molecular interactions.

Some of the commercially available sensor chips are listed and

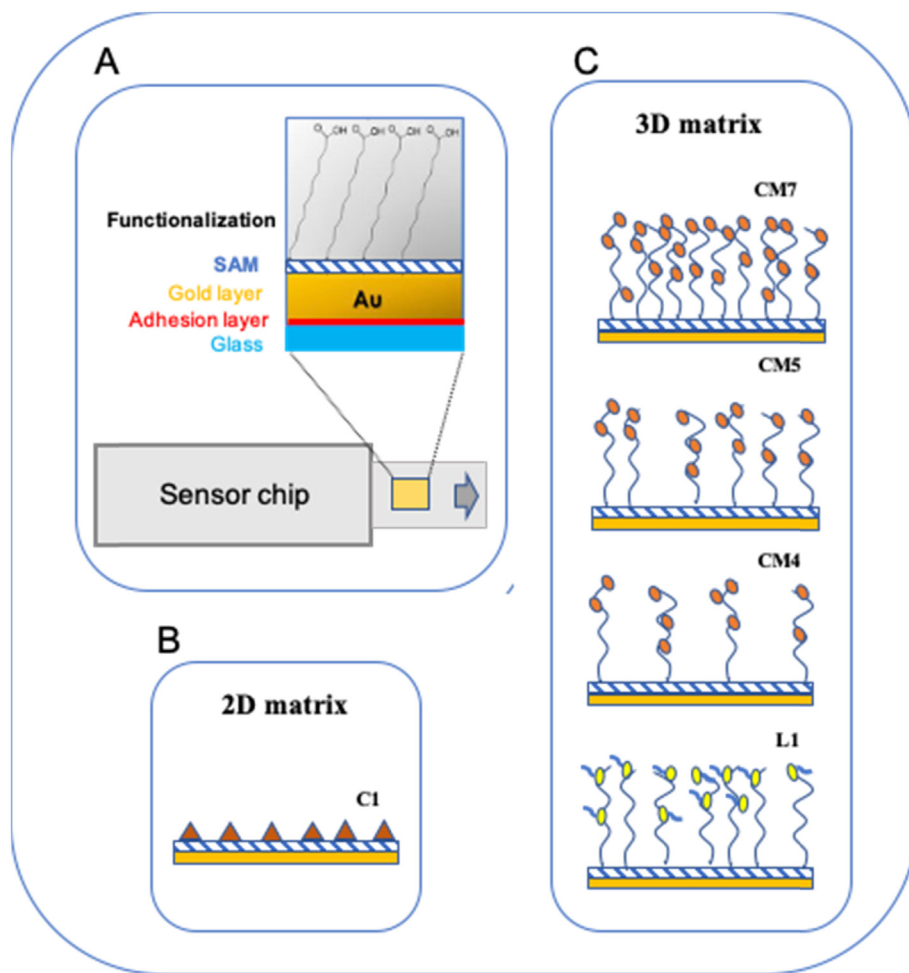


**Fig. 4.** Overview and schematic representation of a sensor chip structure. (A) Layered structure of a SPR sensor chip: glass layer is shown in cyan, adhesion layer in red, gold film in yellow, SAM in blue and functionalized surface in gray (B), (C) Representation of some of the commercially available 2D and 3D sensor chips from Biacore™ with matrix of different capacities.

compared in Table 2. The mentioned manufacturers all use their own techniques to make the sensor chip surface, therefore it is difficult to compare the capacity of the sensor chip directly. More information about sensor chips is available on manufacturers' websites.

### 3.1. Immobilization strategies

The immobilization of the sensing surface is a critical step of the sensing process because a proper selection of the immobilization method should ensure high selectivity and sensitivity. In an SPR experiment, the *ligand* is the bio-recognition element immobilized onto the sensor surface and must maintain its biological activity after immobilization, the *analyte* is the interacting molecule flowing with the experimental buffer [54,55]. Resonance or response units (RUs) are generally used to describe the increase in the signal, where 1 RU is equal to a critical angle shift of  $10^{-4}$  and corresponds to the binding of 1 pg to the surface of a flow cell with the area of 1 mm<sup>2</sup>. The sensor surface must be designed to immobilize a sufficient number of bio-recognition molecules on the sensor while minimizing non-specific binding to the surface [7]. For this reason, despite the importance of the optical configuration and fluidics, the sensor chip can be considered the heart of a SPR instrument.

Theoretically, molecules can be immobilized both directly and indirectly, depending upon the molecular weight of the analyte. For analytes of high molecular weight (greater than 5000 Da), direct binding is used, while the indirect binding is used for low molecular weight analytes [56]. Sensors with planar 2D surfaces (Fig. 4B) are generally based on SAMs, which are modified with small functionalizing groups (e.g. COOH). The flat surface can be useful in experiments involving large analytes such as cells and viruses, although steric hindrance could lead to a lower response if the ligand is immobilized with too high a density.

In contrast, immobilization on a 3D-like matrix typically provides more binding sites and a better environment for storage of the immobilized ligand (Fig. 4C). The three-dimensional surfaces

are modified with compounds including alginate or PEG, but the most used is carboxymethylated dextran [57]. This shows a pronounced tendency to covalent binding due to the presence of this active functional group. Due to their hydrophilic properties, dextrans have a low capacity for non-specific interaction with biological components.

In addition to the 2D and 3D matrices already mentioned, matrices layered on the surface of the metal support are also used in the SPR biosensors. These matrices are composed of layers of silica (SiO<sub>2</sub>) [58], amorphous carbon [59], or graphene [60]. The choice of a strategy for the immobilization of the ligand depends on the type of ligand (protein, sugar, DNA, low molecular mass substance), the analyte to be used (small or large interactors), the purpose of the study (specificity, concentration, affinity, kinetics) and the bioanalytical format selected for the assay (direct, sandwich, competitive, inhibition) [61].

To determine the method of immobilization, any additional information such as the size of the ligand, the isoelectric point, the amino acid composition and the possible orientation of the binding sites is certainly helpful. Generally, the immobilization can occur covalently and therefore be irreversible or by capture and be transient. Depending on the nature of the ligand and the available reactive groups, several covalent coupling chemistries can be selected for the immobilization of the ligand. Among them, the amine (-NH<sub>2</sub>) (Fig. 5), thiol (-SH<sub>2</sub>) and aldehyde (-CHO) coupling chemistries are validated procedures [62,63]. Covalent coupling ensures stability and low consumption of the ligand, which does not need any modification, and whose immobilization level can be easily controlled. Therefore, covalent coupling should be the first choice when evaluating different ways to immobilize biomolecules on a chip surface. However, covalent immobilization can lead to random orientation of the ligand, with the binding sites that can be hidden thus reducing or eliminating the affinity for the analyte [42,64]. Moreover, the low pH or the blocking agent generally used in the immobilization procedure can inactivate the ligand.

Conversely, affinity capturing can be used to reduce or eliminate

**Table 2**

Some of the commercially available sensor chips with description of their surface modifications and specific applications. All of the acronyms used in the table refer to the commercial name as provided by the manufacturer.

Surface Modification	Biacore™	XanTec	Sartorius	Bruker	Creoptix	Applications
	<a href="http://www.cytivalifesciences.com">www.cytivalifesciences.com</a>	<a href="http://www.xantec.com">www.xantec.com</a>	<a href="http://www.sartorius.com">www.sartorius.com</a>	<a href="http://www.bruker.com">www.bruker.com</a>	<a href="http://www.malvernpanalytical.com">www.malvernpanalytical.com</a>	
Short matrix, medium capacity	CM3	CMD50L, HC30 M	–	–	–	Protein - Protein, kinetics
Normal matrix, low capacity	CM4	HLC200 M	–	–	PCL	Assays in serum or culture medium; Positively charged analytes
Normal matrix, medium capacity	CM5	CMD200 M, CMD500L, HC200 M	CDL	–	–	Protein - Peptide/Small molecule; General purpose
Normal matrix, high capacity	CM7	CMD700 M, HC1500 M	CDH, PCH	HCA	PCH	Large ligand-to-analyte molecular weight ratio; General purpose
No matrix, low capacity	C1	CMDP	COOH1	–	PCP	Large analytes and/or cells, viruses, particles, lipid bilayers
Poly His binding group	NTA	NiHC1500 M, NiHC200 M, NiD200 M	HisCap	–	PCH-NTA, PCP-NTA	His-tagged ligands
Hydrophobic surface	HPA	HPP	–	–	–	Model membrane systems
Lipid capturing surface	L1	LD, LP	–	–	PCP-LIP	Hydrophobic ligands: vesicles, liposomes, lipid bilayers, transmembrane proteins
Biotin capturing surface	SA	SAD200 L/M, NAD200 L/M	SADH	Biotin-tag capture	PCP-STA, PCH-STA	Biotinylated ligands; General purpose
PEG-based sensor	PEG	–	–	–	–	Alternative for analytes with unwanted binding to dextran-based surfaces
Protein A, G, L	Protein A, G, L	PAGD, PAGP, PAGHC	–	IgG capture	PCP-PAG	Antibody (IgG) ligands
Plain gold surface	AU	AU	–	–	–	Untreated gold surface for the design of unique surface chemistries

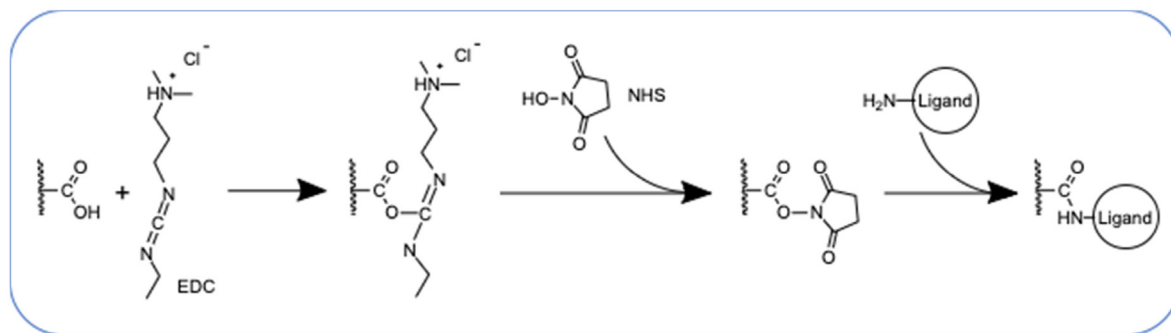


**Fig. 5.** Surface activation with EDC/NHS and amine coupling reaction. EDC N-(3-Dimethylaminopropyl)-N'-ethylcarbodiimide hydrochloride crosslinking protocol includes NHS (N-hydroxysuccinimide) for a two-step reaction: 1. EDC Activates the carboxyl groups and forms an amine reactive O-acylisourea intermediate; 2. The O-acylisourea product intermediate can be easily hydrolyzed, reverting to the original carboxylate molecule. To overcome this limitation, N-Hydroxysuccinimide can be used to form a more stable second intermediate prior to amination.

induced heterogeneity caused by the random coupling chemistries and to prevent the loss of activity for molecules which are sensitive to covalent modification (e.g. binding sites containing free amine groups). In these affinity capturing systems, the binding with the ligand should be strong enough in order to obtain a stable complex. Some of the systems employed for affinity capturing are completely regenerable and a fresh ligand surface can be created with every cycle, in this way the ligand is not required to retain its activity on the surface throughout long assays [61]. Moreover, an additional advantage is that the capturing procedure does not need highly purified samples. However, although such indirect methods appear to be more practical and result in a higher percentage of active ligands after the immobilization procedure, it must be considered that a bulky capturing system occupies a significant fraction of the evanescent field's volume, which is then not available for ligand molecules, thus resulting in smaller signals. Furthermore, the capturing system can alter the affinity profile of the immobilized ligand or induce non-specific interactions [42].

The majority of affinity capturing systems consist of a covalently-bound antibody immobilized using a standard amine coupling procedure [65,66], thus enabling the recognition of several types of antigens. Among them, the polyhistidine, the myc, the GST, the MBP and the FLAG tags represent the most widely used functional groups [30,67].

A different approach involves the modification of the sensor chip surface to capture special tags. For instance, biotinylated ligands can be directly immobilized with high affinity on commercially available streptavidin-coated sensor chips [68]. Furthermore, the presence of a six histidines tag allows the capture of a protein with the nitrilotriacetic acid (NTA) groups of the sensor surface. The NTA molecule chelates metal ions such as Nickel ( $\text{Ni}^{2+}$ ), creating coordination sites that bind to poly-histidine tags on recombinant protein and other biomolecules. Finally, modifying the sensor chip surface with a hydrophobic compound makes it possible to capture vesicles. The immobilized vesicles can be used to insert proteins with hydrophobic regions (e.g. membrane proteins), which are otherwise challenging to immobilize without losing their biological activity [30].

A summary of the above-mentioned immobilization strategies with the list of the related suitable ligand types is reported in Table 3.

When the immobilization process is completed, the solution containing the analytes can be injected over the immobilized ligand. The binding process, by increasing the mass at the chip surface, induces a change in refractive index of the area surrounding the metal dielectric interface; hence, the resonance condition is deviated and can be observed as a change in signal

corresponding to the shift of the resonance angle. When RUs are plotted *versus* time, a sensorgram is produced (Fig. 6).

#### 4. Experimental optimization and data analysis

The main goal of a SPR experiment is to determine the kinetic constants of a label-free biomolecular interaction by fitting the sensorgram to a kinetic model using a mathematical algorithm. Unfortunately, fitting the line through a data set is not always easy and cannot be entrusted to a mathematical model but it is often necessary to proceed on the basis of personal experience, chemical knowledge and structural information of the target. In addition, surface effects, such as immobilization heterogeneity or cross-link and mass transfer effect or analyte rebinding, can significantly affect the data [69,70]. Thus, in order to improve the experimental design and to achieve high quality interaction data, there are a number of tips that must be considered.

For instance, in some cases it is important to reduce the quantity of ligand immobilized on the sensor chip in order to minimize the effect related to mass transport, aggregation and overcrowding. Mass transport is defined as the transport of an analyte from its bulk solution to the sensor chip surface. When this transport is slower than the association rate constant ( $K_{on}$ ) of the binding system, the binding kinetics will be mass transport limited, resulting in an inaccurate measurement which can be sometimes identified on the sensorgram as an association phase with lack of curvature. To prevent such an artifact, besides the reduction of immobilized ligand, the increase of analyte flow rate and the choice of appropriate analyte concentration should be also considered [71,72]. The highest flow rate which is compatible with the analyte injection time must be selected for the assay. To assess the existence of mass transport effect, a single analyte concentration should be injected at several different flow rates. Indeed, the mass transport effect is influenced by flow whereas the intrinsic reaction rate is flow independent. Therefore, only in the case that the association and dissociation rate constants are not affected by the flow rate variation, the mass transport limitation can be excluded. The analyte concentrations throughout the experiment should be well spaced out, covering a range between 0.1X and 10X the expected  $K_d$  of the interaction when it is known (as an example, for an interaction with an expected  $K_d = 10$  nM, concentrations from 1 to 100 nM are appropriate) [73]. In addition, with the aim to properly calculate kinetics, the binding must be analyzed using at least five separate analyte concentrations, which can reach the number of eight/ten when performing steady-state affinity analysis.

Regeneration of the ligand between each analyte injection is a further fundamental operation to obtain reliable data. Regeneration



**Table 3**  
Main suitable immobilization strategies for different types of ligands.

Immobilization strategy	Method	Ligand type	Advantages	Disadvantages
Covalent coupling (irreversible)	Amine coupling (most generally applicable coupling)	Proteins Peptides Small molecules Carbohydrates Glycoproteins DNA	High coupling yield Stable bond Does not require any modification of the ligand Low ligand consumption Immobilization level easily controlled	Random ligand orientation (non-uniform coupling) Partial/complete ligand deactivation or damage
	Thiol coupling	Proteins Antibodies Glycoproteins		
	Aldehyde coupling	Carbohydrates Glycoproteins		
Capturing (transient)	Streptavidin–Biotin coupling	Proteins Antibodies Glycoproteins Peptides Oligonucleotides	Oriented coupling Retention of the ligand's activity and structure Regenerable Does not require highly purified samples	Unstable bond Capturing system can interfere with the function or binding site of the ligand Smaller signals
	NTA-Ni <sup>2+</sup> - His <sub>6</sub> complexes	Proteins Antibodies Peptides		Non-specific interactions
	capture antibodies	Almost any proteins, including membrane proteins ( <i>via</i> tags) Cells Viruses		
	Protein A/G Hydrophobic surface	Antibodies Vesicles Liposomes		

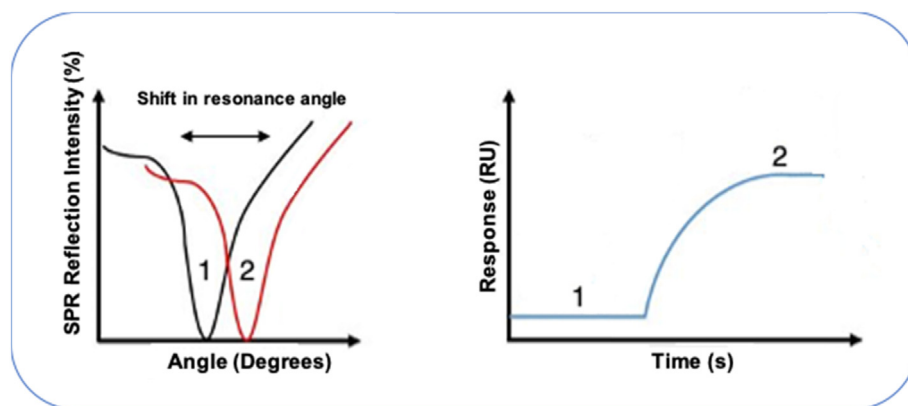


**Fig. 6.** Spectrum of reflected light before (1) and after (2) refractive index change caused by the molecular interaction on the chip surface.

has the function of totally removing the analyte without irreversibly damaging the immobilized ligand [74] and it is a must when the dissociation is very slow. This procedure has to be evaluated empirically, since the combination of physical forces responsible for the binding are often unknown. As the regeneration solution needs fewer gentle conditions to break the interactions, it is important to check the baseline after regeneration and perform control injection to monitor the possible degradation of the ligand.

A further common artifact that can be found in an SPR experimental curve can be ascribed to the non-specific binding, which can occur when the analyte interacts with the surface instead of the ligand. A number of experimental methods are often used to reduce non-specific binding, such as increasing salt concentrations, adjusting buffer pH and adding surfactants. Moreover, most sensor chips in use have many channels through which the analyte is passed and one of them is typically used as a reference channel [75]. Reference subtraction serves to exclude artifacts associated with the injection to compensate for non-specific binding to the sensor chip and also for bulk refractive index differences between

flow buffer and analyte sample, which represents an additional issue in an SPR assay. In some cases, particularly when a high-RI solvent such as DMSO is used to dissolve the analytes, giving rise to large shifts in RI during the injections, and simple subtraction of the signal from the reference channel is no longer enough, a DMSO calibration curve can be constructed by injecting the solvent with varying concentrations and used for correcting response levels obtained during sample injections [76].

After reference subtraction, large spikes can appear both at the beginning and at the end of the injection. This happens because in many instruments the flow channels are in series and the sample rate deviates slightly and generally can be minimized by using a reference subtraction function usually included in the data analysis software.

Many blank injections, which correspond to the zero concentration of the analyte, are also recommended to prime the system at the beginning of an experiment, and waiting for the system to equilibrate is advisable before starting a new assay. The baseline should be practically flat before any experiment can start [77].

As soon as the blank signal is stable, the closest blank for each injection or the average of overall blank injections can be used to compensate for the drift and small differences between the reference and active channel.

The reference subtraction and the blank subtraction are often referred to as *double referencing*, which allows to compensate for the differences between the reference and the active channels [77,78].

Furthermore, as with any analytical technique, good quality data can only be obtained with instruments that are in perfect working order [79] and it is highly recommended to perform the binding experiments in duplicate or even in triplicate. In this way, a standard deviation for the kinetic results can be obtained to evaluate for goodness of the measured data.

While it can be relatively simple for SPR users to obtain binding signals in their experiments, a rational experimental design seems to be of crucial importance for achieving high-quality data. Moreover, tools for the analysis of SPR data are very limited in their ability to correct for poorly designed assays [80]. After an accurate evaluation of the experimental conditions, some tools such as KD-Assistant, SPR-Simulation, BIACalculation and BiaMethodwriter can be very helpful in the initial stage of assay development and optimization. These platform-independent packages can generate theoretical response curves and time to equilibrium, and calculate analyte concentrations, sample volumes and experiment run times necessary to achieve the desired signals. In addition, these tools are available for free or for a small fee [81], giving the opportunity to explore assay design in more detail and to allow the importation of data for platforms lacking in machine-specific software.

Due to the variety of instrument configurations and to usage restrictions imposed by manufacturers, many of the software packages in use for the data analysis are platform specific and they exist independent from the software for instrument control and data collection, so that data analysis can be accomplished while an assay is being actively run [80]. Besides the preconfigured software tools, third-party software can also be used with an instrument's specific hardware and database format. Among them, Scrubber (Biologic Software), TraceDrawer (Ridgeview Instruments), Screener (Genedata) and CLAMP (University of Utah) [78] are examples of instrument-independent analysis tools that can be employed with many different commercial platforms. Additional information about the software, their application and their compatibility on different SPR platforms can be found on developers' websites.

Recently, the workflow concept, design and experiences with a software module depending on a browser-based software platform for the processing and the analysis of SPR data has been presented [82]. Among others, this novel solution showed great benefits in terms of time saving thanks to the experimental templates and the automatic data reporting, increased consistency and visibility because all data are analyzed in the same way, and reduced training and infrastructure burden since updates to the SPR module are applied on a server environment and become available immediately to all users.

## 5. Case studies

SPR is not limited to monitor protein-protein interactions, but it also allows to investigate the binding of a protein towards small molecules in the drug discovery process as well as the interactions between DNA–DNA, DNA-protein, lipid-protein and hybrid systems of biomolecules and even non-biological surfaces. As a consequence, biomolecular interaction analysis can be used in a number of ways: *i*) for the identification of the binding between two or more interactants, *ii*) for the determination of the affinity of

the interaction, *iii*) for measuring the actual association and dissociation rates, *iv*) for the quantification of the concentrations of one of the interactants and *v*) for high-throughput screening of druggable molecules [30,45].

In the following section, different case studies are described, according to the diverse approaches including *i*) the study of the conformational structure of macromolecules and their interactions, *ii*) sensing, and *iii*) drug discovery. The reported case studies were selected mainly based on our experience with the aim to guide the user through the situations that most commonly occur. Furthermore, this paragraph represents an overview of the various difficulties that may be encountered in the use of SPR technology and offers an explanation of the various issues and tricks for overcoming them. For in-depth information, the reader is referred to the literary source. In order to make the described experimental conditions potentially reproducible, only case studies in which commercial sensor chips were used are described.

A summary of the experimental strategy used in the case studies described below is reported in Table 4.

### 5.1. CASE 1: screening of biomolecules

This case study has been selected as the first example of the use of SPR technology whose basic application is represented by the screening of a more or less large set of molecules. The study of the binding affinities towards a given target allows for gaining important structural information for the optimization of biomolecules in the drug-design process.

In this case study we take in consideration a series of purified saponins and sapogenins whose affinity was tested towards the Peroxisome Proliferator-Activated Receptor gamma (PPAR $\gamma$ ), a nuclear receptor considered as a master regulator of adipogenesis in mammals [83,84], in order to select the most promising compounds for X-ray analysis [85]. To this end, we followed a two-stage scheme: in the first stage we quickly selected the best candidates, in the second we clearly defined the binding features of the molecules selected. For the initial fast screening, a Pioneer SensiQ with One-Step $\text{\textcircled{R}}$  gradient injection technology was used [33]. This method allows to determine the kinetic and affinity parameters of a binding interaction by using only a single analyte gradient injection. When this method is used, the advantages are that the sample has only one known concentration and is dispersed through a volume of running buffer as it is flowed to the sensor chip surface. In addition, with respect to the traditional screening approaches, OneStep $\text{\textcircled{R}}$  enables the same analytical performances in a time-saving manner. This method, based on Taylor dispersion, produces a sigmoidal concentration gradient of analyte in the capillary fluidic line (Fig. 7A). As the sample gradient flows from the capillary to the sensor chip, binding data are collected in real time incorporating the full range of analyte concentrations presented to the surface from low to high. Two of the tested compounds (saponins 18 and 19) showed considerable affinity for PPAR $\gamma$  Ligand Binding Domain (LBD) and then tested according to a traditional multi-cycle kinetic (MCK) analysis of biomolecular interactions and different concentrations of analyte in solution binding to the immobilized ligand were used. The affinity ( $K_d$ ) and rate constants ( $k_{on}$ ,  $k_{off}$ ) for the interaction between PPAR $\gamma$  LBD and the selected saponins are reported in Fig. 7D and compared with the reference agonist LT175 [86].

From the analysis it has emerged that compound 18 showed a unique binding profile if compared with all the other tested compounds (Fig. 7B) and the data obtained from kinetic analysis of saponin 18 were more suitable for a 2:1 molecular interaction model, suggesting that two molecules could bind the receptor LBD at the same time. In addition, the high affinity binding site showed

**Table 4**  
Schematic representation of the described case studies with the experimental strategy used.

PURPOSE	SENSOR CHIP	INSTRUMENT	ANTIBODY	IMMOBILIZATION STRATEGY	LIGAND DENSITY (RUs)	FLOW RATE ( $\mu\text{l}/\text{min}$ )	ASSAY BUFFER	Ref.
<b>CASE 1</b> Screening of biomolecules	PCH Normal matrix, high capacity	SensiQ Pioneer AE	NO	Amine-coupling	13,500	50	HBS with 1 mM DTT and 2% DMSO.	[85]
<b>CASE 2</b> GPCR-analyte interaction	PCH Normal matrix, high capacity	SensiQ Pioneer AE	anti-His <sub>6</sub>	Amine-coupling + capturing	500	25	HBS with 0,03% DDM/CHS (5:1)	[88]
<b>CASE 3</b> Competition	PCH Normal matrix, high capacity	SensiQ Pioneer AE	NO	Amine-coupling	14,000	150	HBS with 0,005% P20 and 1% DMSO	[109]
<b>CASE 4</b> Multiple binding sites	PCH Normal matrix, high capacity	SensiQ Pioneer AE	NO	Amine-coupling	15,000	75	HBS with 0,005% P20, 1 mM DTT and 2% DMSO.	[97]
<b>CASE 5</b> Avidity	CDL Normal matrix, medium capacity	SensiQ Pioneer AE	NO	Amine-coupling	175	75	HBS with 0,005% P20	[102]
<b>CASE 6</b> Competitive immunoassay for Cd <sup>2+</sup> detection	CM5 Normal matrix, medium capacity	Biacore XTM	anti-Cd <sup>2+</sup>	Amine-coupling	2526	10	HBS with 0,005% P20 and 3 mM EDTA	[114]

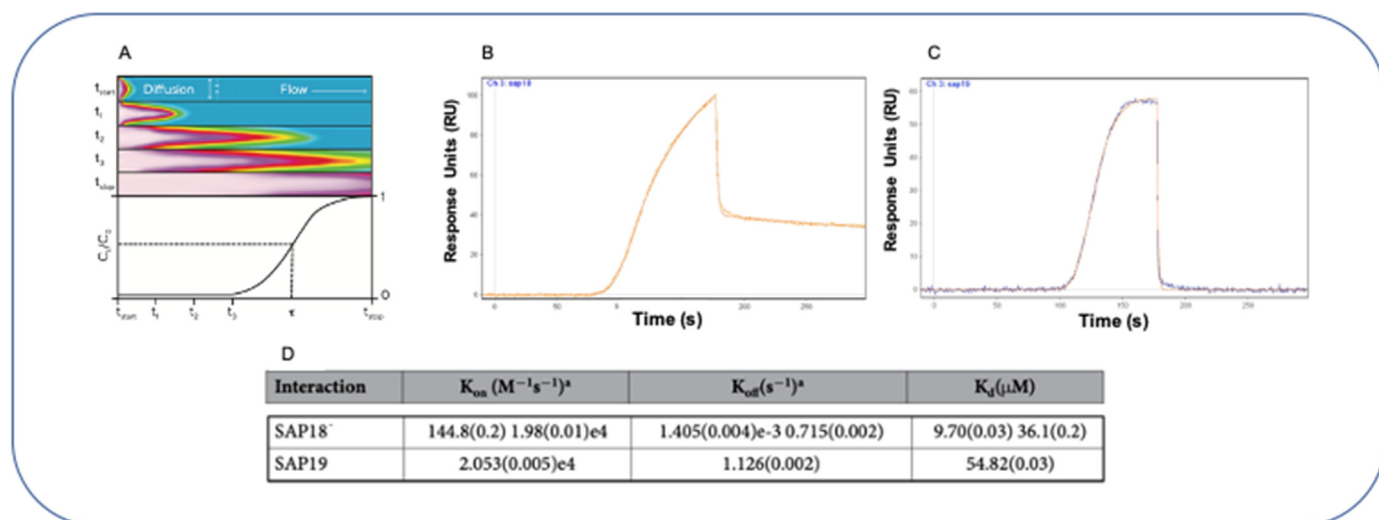


**Fig. 7.** Kinetic analysis of saponins binding to PPAR $\gamma$  LBD using OneStep<sup>®</sup> injection (A) OneStep<sup>®</sup> gradient formation in the injection line (top panel), with the corresponding analyte concentration measured within the flow cell (bottom panel). The running buffer is represented in blue and the analyte dispersion is represented in pink. The gradient formation and its relationship to analyte concentration at the flow cell are illustrated using five simulated snapshots ( $t_{start} - t_{stop}$ ) of the injection line at different times, showing that a single injection can be used to test a full analyte concentration series. (B) The global fit of the data to a 2:1 bimolecular interaction model for compound 18 and (C) a 1:1 model for compound 19 are represented. (D) Kinetic parameters of LT175, SAP18 and SAP19 obtained with the OneStep<sup>®</sup> injection method. For LT175 and SAP18, data were fit to a 2:1 molecular interaction model. Experimental error is reported in parentheses.

a very small kinetic association rate constant  $k_{on}$  compared to that of the other compounds ( $144.8 \text{ M}^{-1}\text{s}^{-1}$  versus values ranging from  $1 \cdot 10^3$  to  $6.1 \cdot 10^4 \text{ M}^{-1}\text{s}^{-1}$ ) and a lower dissociation rate constant  $k_{off}$  ( $1.4 \cdot 10^{-3} \text{ s}^{-1}$  versus  $0.69\text{--}4.13 \text{ s}^{-1}$ ), therefore slow kinetics of association and dissociation can be hypothesized. Indeed, similar behavior has been previously described for other nuclear receptor antagonists [87]. By contrast, the sensorgram of compound 19 showed a rapid association and dissociation time (Fig. 7C). SPR analysis also evidenced that the presence of a methyl or alcoholic group in position C-23 on the triterpene nucleus conferred greater affinity to the molecule, while a carboxyl group in the same position produced the opposite effect.

## 5.2. CASE 2: membrane proteins

One unfilled gap in SPR technology remains the lack of a methodology for the effective immobilization of membrane proteins on the sensor chip. Indeed, because of the intrinsic instability of these latter when extracted from the lipid environment, only few examples of successful processing have been reported so far, making them very challenging objects for SPR techniques.

In this case study, an experimental strategy aimed to characterize the interaction of the membrane G Protein-Coupled Receptor (GPCR) GPR17 with analytes and specific antibodies have been proposed [88]. As the measure of the binding kinetics and affinities

of analytes to intact membrane proteins by SPR is a challenging mission, the method here described represents an easier alternative that consists in the exploitation of the presence of a tag, such as poly-histidine or a short peptide sequence, bound to the protein to be immobilized. Indeed, the detergent-solubilized receptor engineered with a tag, could be efficiently captured with a specific antibody previously covalently immobilized onto a chip [89]. This allows to overcome many problems mainly related to the intrinsic difficulties in immobilizing membrane proteins on chip surfaces while retaining their native conformation [90–92] either in the original membrane environment or in membrane-mimicking structures, such as for example, lipid bilayer disks [93]. In the case described here, 18000 RUs of a specific antibody for His<sub>6</sub>-tagged proteins were covalently immobilized on the three channels of the chip surface using standard amine coupling chemistry, then the solubilized GPR17 receptor was captured.

To this end, an aliquot of the crude membrane extract was prepared according to the procedure reported in the paper and injected across the PCH sensor chip where the anti-His<sub>6</sub> antibody was previously immobilized. In order to remove non-specifically bound supernatant debris, the chip surface was washed for several hours with the running buffer. Alternatively, a few short injections of 0.5 M NaCl showed to be similarly effective to this purpose. After the washing procedure, the receptor was captured on two out the three channels of the sensor chip, using the third channel as reference. When necessary, a regeneration solution was used to completely remove the receptor from the sensor chip surface, so that the immobilized antibody was ready for capturing freshly solubilized GPR17 for new experiments. This regeneration procedure is of great advantage, given the intrinsic instability of the membrane proteins out of their lipid environment. The SPR results obtained with the high affinity antagonist Cangrelor and the agonist Asinex 1 demonstrated that the immobilized GPR17 retained its ability to specifically bind the analytes.

The sensorgrams concerning the full kinetic analysis with the

agonist Asinex 1 and the antagonist Cangrelor binding to GPR17 are shown in Fig. 8A and B, respectively, with calculated binding parameters listed in Fig. 8C. Although the affinity ratio between Cangrelor and Asinex 1, as measured by SPR, is consistent with previous literature [94–96], the absolute  $K_d$  values obtained from the SPR experiments are notably higher. This discrepancy could be attributed to residual non-specific binding to GPR17, likely caused by the injection of crude membrane preparation, which could potentially influence the calculated  $K_d$  values. Furthermore, it is important to note that a perfect correlation cannot be expected because SPR provides direct binding data, while the literature data are derived from a different functional assay [95,96]. In addition to influencing the affinity constant, the injection of the crude extract also affects the amplitude of the signal because of the presence of cellular debris that reduces the concentration of the active receptor on the sensor chip. As a consequence, all the signals generated from the analyte binding are included within an interval of few RUs, thus lowering the noise-to-signal ratio and making it more noticeable (Fig. 8A and B).

### 5.3. CASE 3: multiple binding sites

SPR technology can be usefully employed to identify or rule out the presence of multiple binding sites within the ligand binding domain of a given protein. To this end we have taken as an example a work of Montanari et al. [97], where the authors demonstrated that the ligand LT175 was responsible for the allosteric inhibition of the phosphorylation of nuclear receptor PPAR $\gamma$  LBD at Serine 273 mediated by the protein kinase Cdk5 [98]. To exclude the possibility that such inhibition was caused by the binding of LT175 to an alternative binding site instead of the canonical one, an SPR experiment was set-up. Indeed, some PPAR $\gamma$  ligands are known to bind an alternative low affinity site, especially at high concentrations [99,100]. At this purpose, PPAR $\gamma$  LBD was preventively complexed with the small ligand GW9662 (Fig. 9B and C), known to

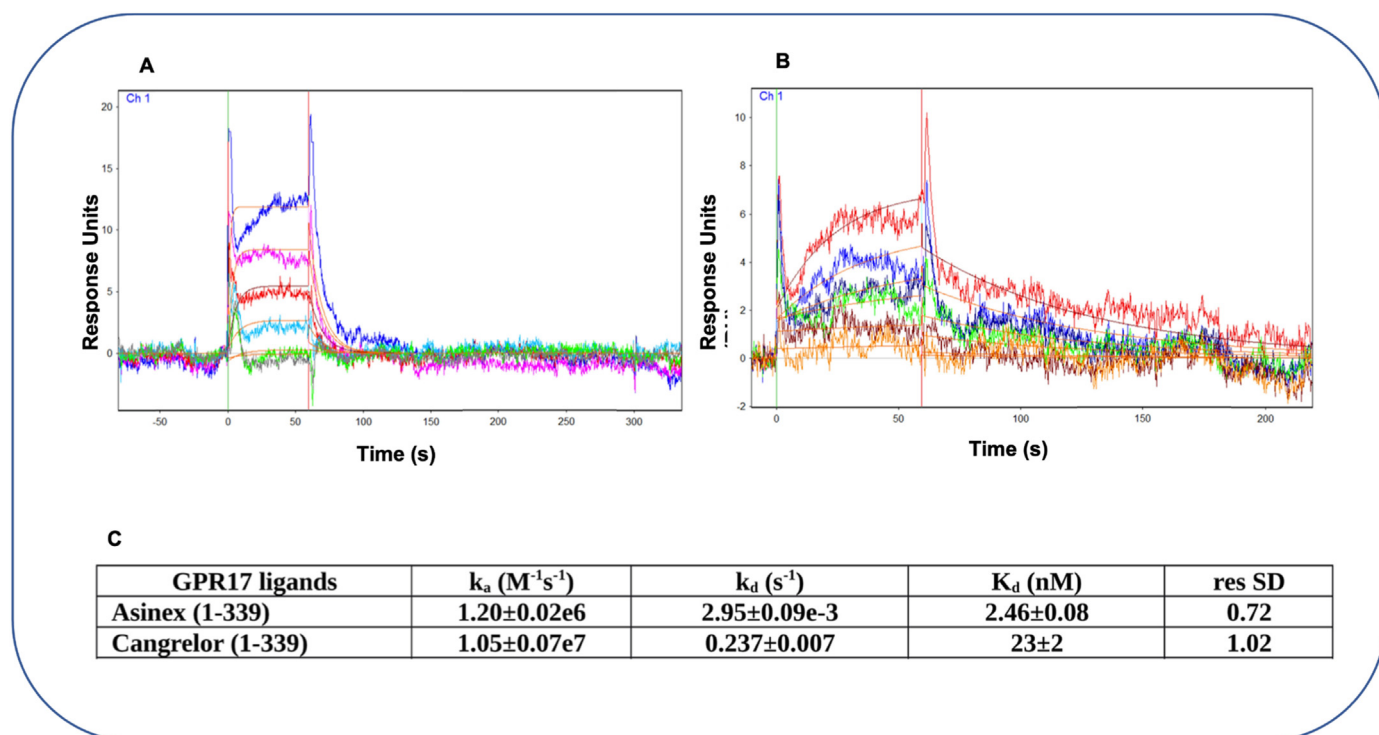
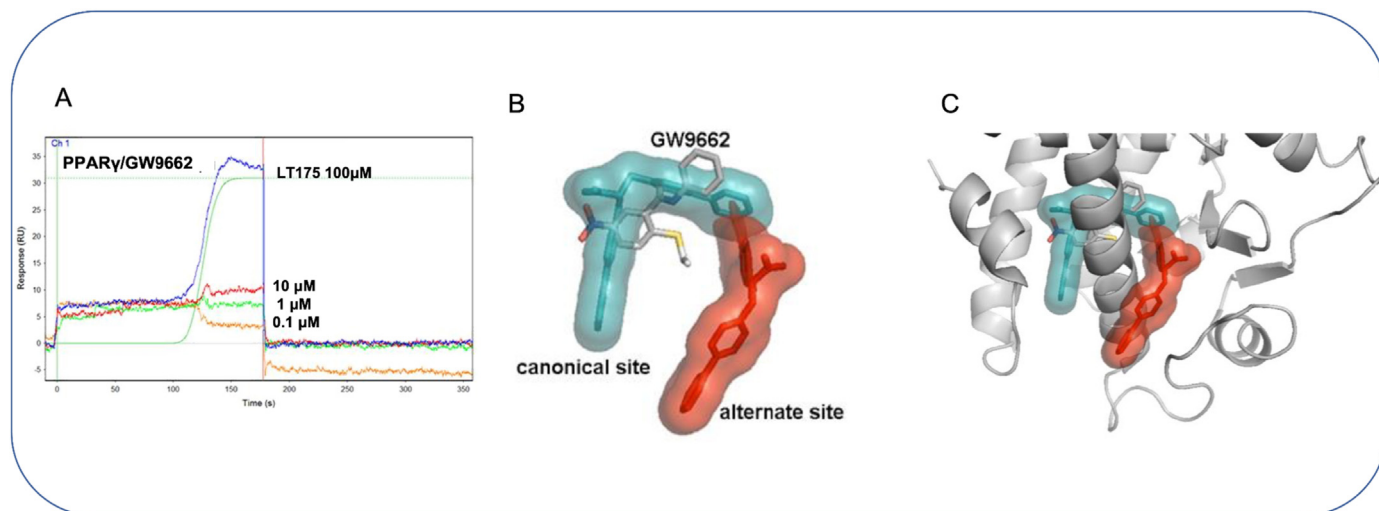


Fig. 8. Full kinetic analysis of the agonist Asinex 1 (A) and the antagonist Cangrelor (B) binding to GPR17, with the determined binding parameters listed in table (C).



**Fig. 9.** (A) Sensorgrams superposition of LT175 injected using OneStep® at four different concentrations (gradient injections from 0 up to 0.1, 1, 10 and 100  $\mu\text{M}$ ) over immobilized PPAR $\gamma$  LBD pre-complexed with the covalent antagonist GW9662; (B, C) Structure superposition of GW9662 (light gray; PDB code 3B0R) and LT175 (cyan) in the PPAR $\gamma$  LBD. The alternate site, occupied by a modeled molecule of LT175 (red), is also shown.

covalently bind the nuclear receptor LBD in the same binding region as LT175 (at residue C285) [101]. Then, the complex PPAR $\gamma$  LBD/GW9662 was immobilized on the sensor chip and LT175 was injected into the flow cell at different gradient concentrations (from 0 up to 0.1, 1, 10, and 100  $\mu\text{M}$ ) using the OneStep® injection method [33]. The sensorgrams in Fig. 9A showed that only at the highest concentration of 100  $\mu\text{M}$ , LT175 was able to bind a lower affinity alternate binding site.

#### 5.4. CASE 4: avidity

Protein aggregation on the chip surface may lead to a reduction in active material or in the average number of exposed epitopes per immobilized mass. As a consequence, the binding affinity is underestimated.

In this case study, SPR was used as a powerful tool to provide evidence that the three proteins involved in *de novo* Deoxythymidine monophosphate (dTMP) synthesis assembled to form the thymidylate synthesis complex (dTMP-SC) in the cytoplasm and not only after nuclear translocation, as it was assumed [102].

To this aim the dTMP synthesis complex was successfully assembled *in vitro*, employing tetrameric serine hydroxymethyltransferase (SHMT1) and a bifunctional chimeric enzyme comprising human thymidylate synthase (TYMS) and dihydrofolate reductase (DHFR). A chimeric fusion polypeptide (Chimera) including both proteins (TYMS and DHFR) was then designed and assessed the formation of dTMP-SC between Chimera and SHMT1.

To evaluate the binding affinity SPR experiments were performed. Chimera was immobilized onto the sensor chip and tetrameric SHMT1 was used as the analyte and injected at different concentrations (85, 42.5, 21.2, 5.3 and 2.66  $\mu\text{M}$ ) (Fig. 10A). Even though the precise stoichiometry of the putative complex was unknown, the higher symmetry of SHMT1 suggested that two Chimera dimers (DFHR-TYMS:TYMS-DHFR) may bind to one SHMT1 tetramer. In this case, the tetrameric form of SHMT1 would have two identical binding sites. This would allow the analyte to bind first with one site to the ligand Chimera and then to bind to another Chimera molecule in close contact to the second ligand site. The second binding event will give a stabilization of the ligand-analyte complex without extra response but shifts the

equilibrium constant to a more stable interaction. This effect, which is often referred to as *avidity* (Fig. 10B) [103,104], was observed in the case of SHMT1 binding to Chimera, suggesting that indeed SHMT1 may bind more than one Chimera dimer. A bivalent analyte gives rise to two sets of rate constants, one for each binding step, although the meaning of the two sets of rate constants and particularly the second set is very difficult to interpret. However, the avidity effects can be reduced using very low ligand levels and high analyte concentrations. Low ligand levels give a sparsely distributed ligand on the chip, with less chance of two ligand molecules being within reach of a single analyte. On the other hand, a high analyte concentration competes out the second binding site, favoring the formation of a 1:1 complex. For this reason, a very low immobilization density of the ligand (175 RUs) and high analyte concentrations were used in this experiment. In this way, the avidity effect was minimized and a 1:1 bimolecular interaction model to fit the experimental curves and estimate an initial value for the  $K_d$  of 2.5  $\mu\text{M}$  and 2.9  $\mu\text{M}$  on channel 1 and 3 of the sensor chip, respectively, was used. This data showed that the interaction between Chimera and SHMT1 was specific, and that the dissociation constant was in the low micromolar range (Fig. 10C).

#### 5.5. CASE 5: protein-protein interaction and surface competition: the importance of the flow rate in the induced fit inhibition mechanism

In this case study we explored the importance of the flow rate as an advantageous strategy to prevent nonspecific binding when dynamic structural elements of the protein can affect the binding of the molecules.

AURKA, a member of the Aurora Kinases family, is a Ser/Thr kinase involved in the progression of mitosis. AURKA is widely overexpressed in a variety of solid tumors [105]. In particular, in neuroblastoma, a severe childhood cancer that arises from highly proliferative migratory cells of the neural crest [106], AURKA is highly expressed relative to normal tissues, and also displays a critical function by binding to and stabilizing the oncoprotein N-Myc [107].

In neuroblastoma cells, the mitotic kinase Aurora-A (AURKA), prevents N-Myc degradation by directly binding to a highly

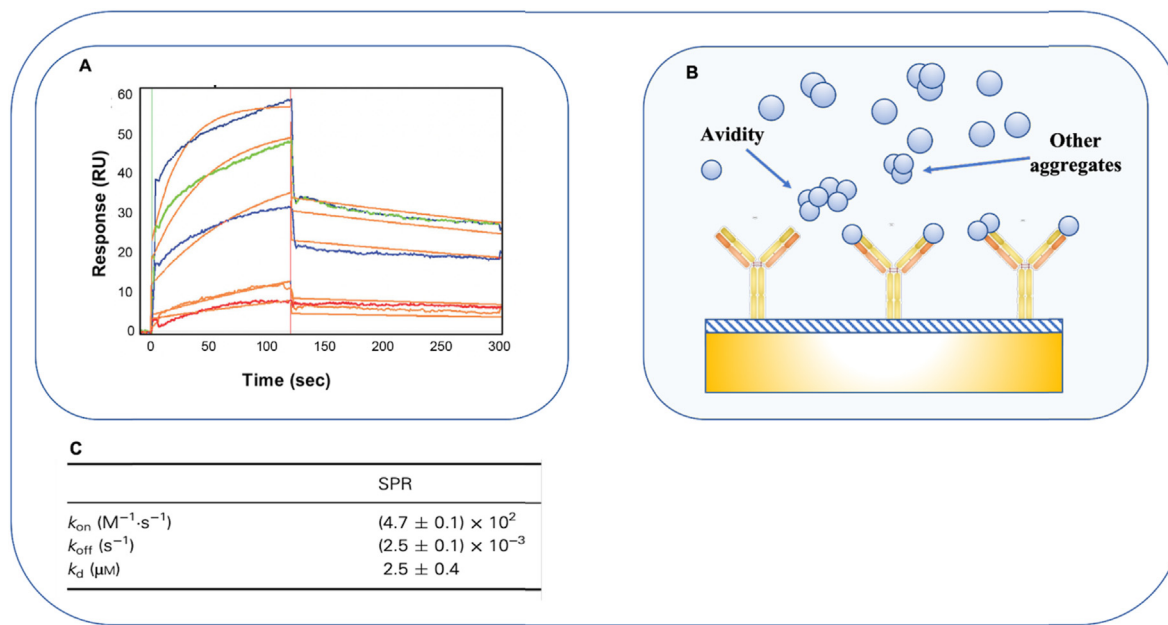


**Fig. 10.** (A) Full kinetic analysis of SHMT1 binding to Chimera at different concentrations. Orange lines represent the global fits of the data to a 1:1 bimolecular interaction model; (B) Schematic representation of *avidity*: inactive aggregates decrease the effective monomer concentration, while multivalent aggregates lead to avidity; (C) Kinetic binding parameters calculated by SPR.

conserved N-Myc region [108]. As a result, elevated levels of N-Myc are observed. During recent years, it has been demonstrated that some ATP competitive inhibitors of AURKA also cause essential conformational changes in the structure of the activation loop (A-loop) of the kinase by inducing a complete flip of the activation loop, retaining it in a “closed” conformation not able to bind N-Myc, thus impairing the formation of the AURKA/N-Myc complex. In this study, the ability of several compounds to disrupt the interaction between AURKA and the AURKA interacting region of N-Myc (Myc-AIR) *in vitro* has been assessed using SPR surface competition assays [109]. In such a type of assay, the primary target (AURKA) is immobilized onto the sensor surface, while the analytes that compete with each other for the binding with the ligand are

dissolved in the running buffer and injected over the chip surface simultaneously (Fig. 12A).

First, AURKA was immobilized onto a high capacity sensor chip and full kinetic analysis was performed for Myc-AIR ( $K_d = 990$  nM; Fig. 11A) and for all the inhibitor compounds (Fig. 11D) by injecting increasing concentrations in the running buffer. In this case, the dynamic A-loop conformation affected the binding of the inhibitors. In order to minimize this effect, the experiments were carried out at a fast flow rate of  $150 \mu\text{L min}^{-1}$ . Then, in order to evaluate the ability of the inhibitors to interfere with Myc-AIR binding to AURKA, a surface competition assay of Myc-AIR in the presence of a saturating concentration (at least 10-fold higher than calculated  $K_d$ ) of each inhibitor was performed. Tested inhibitors

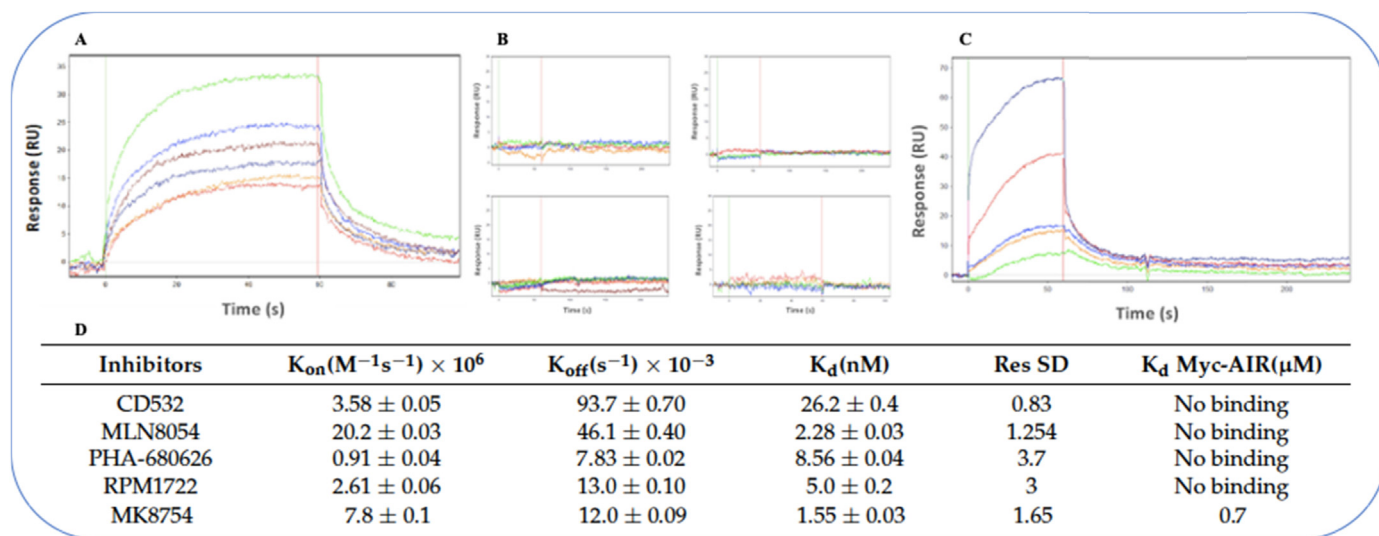


**Fig. 11.** (A) Sensorgram of Myc-AIR binding to AURKA; Kinetic data for Myc-AIR:  $K_{on}$ ,  $6.3 \pm 1 \cdot 10^4 M^{-1}s^{-1}$ ;  $K_{off}$ ,  $0.0659 \pm 0.0008 s^{-1}$ ;  $K_d$  990 nM; Res SD 2.17; (B) Sensorgrams of competition experiments between the inhibitors and Myc-AIR showing complete inhibition; (C) Sensorgram of competition experiment between the negative control compound MK8754 and Myc-AIR; (D) Kinetic parameters of the tested compounds.

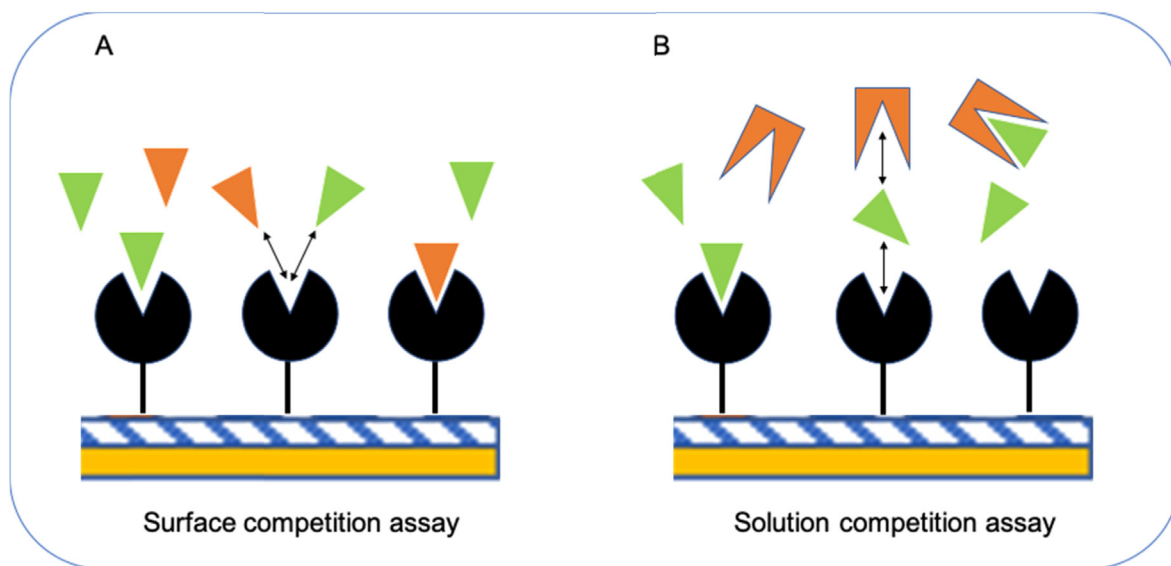


**Fig. 12.** Schematic representation of two possible strategies for competition assays. (A) In the surface competition assay, the molecule of interest and a known third-party binder compete with the same binding site of the primary target which is immobilized on the sensor surface. (B) In the solution competition assay, the primary target and the molecule of interest are injected together, while the know-third party binder is immobilized. In this way, the competition for the binding with the primary target occurs in the solution.

almost completely prevent Myc-AIR from binding to AURKA (Fig. 11B), while such an interaction remained unchanged ( $K_d$  690 nM; Fig. 11C) upon competition with negative control compounds MK8754. Thus, SPR data confirmed the behavior of the investigated inhibitors as Conformational Disrupting compounds.

#### 5.6. CASE 6: solution competitive immunoassay for the detection of $Cd^{2+}$ in water samples

Cadmium is one of the most toxic heavy metals for human beings with great environmental and health impact. At the present time, cadmium can be determined by some classical and modern analytical methods, such as atomic absorption spectroscopy (AAS) [110], inductively coupled plasma mass spectrometry (ICP-MS) [111], non-thermal Optical Emission Spectrometry (OES) [112], and miniature dielectric barrier discharge optical emission spectrometry (DBD-OES) [113]. Although these methods are sensitive and accurate for the detection of Cadmium, they have considerable disadvantages such as longer consumption times, increased technical expertise and tedious sample pretreatments. Moreover, some labeling methods are not suitable in some cases, because labeling materials may occupy important binding sites or cause steric hindrance, resulting in inaccurate data. In this case study a CM5 sensor chip was used as a sensing surface for detecting  $Cd^{2+}$  on a Biacore system, showing how SPR technology, through the immunological detection strategy based on antigen–antibody interaction already described for the detection of biological samples, could be used as a new method for the detection of pollutants [114]. In the case study described, the authors report for the first time a specific and sensitive competitive SPR immunoassay for the detection of cadmium ( $Cd^{2+}$ ) in water samples. In this competition assay format, the primary target (anti- $Cd^{2+}$  antibody) and the molecule of interest ( $Cd^{2+}$ ) are dissolved and injected in the running buffer, whereas a known third-party binder (antigen) is immobilized onto the sensor surface. In this way, the competition for the binding with the primary target occurs in the solution where the target is dissolved into (Fig. 12B), instead of the sensing surface as previously described for the case study 3. At present, all antibodies specific for cadmium recognize  $Cd^{2+}$  only in the chelated form Cd–EDTA. Because of the

competition of the antibody with the high concentration of  $Cd^{2+}$  in the solution for the antigen, the SPR response change decreased due to the less amount of the antibody bound on the chip surface (Fig. 13). Combining the specific monoclonal antibody with the sensitive and label-free analytical SPR method, the SPR based immunoassay was able to rapidly detect  $Cd^{2+}$  with high sensitivity and specificity. In this work, the authors performed *in situ* detection experiments of  $Cd^{2+}$  in real aqueous samples collected from Wenyang Lake in Datong city, providing a novel theoretical and technical support for the detection of heavy metal ions that can be extended in the future as a useful model for the detection of other small molecular compounds in biological, food and environmental areas.

## 6. Future perspectives

It is not surprising that the growth of the SPR market is witnessing a positive outlook in the years to come and it is clear that the SPR technology still has great margins for its evolution. In particular, so far SPR technology has been effectively used only for laboratory analysis but the versatility of this technique makes possible the emergence of new strategies aimed at providing new solutions routinely applicable (*i.e.* as personal healthcare devices and for testing contaminants in drinking water and food or as well as a first hand tool for the characterization of injectable biofluids prior to use). The use of sensors capable of monitoring more than one parameter at the same time, for example for diagnostic use as Point of Care (POC) or for a rapid semi-quantitative preliminary screening of final products for allergic consumers, has long been the focus of market players [115,116]. To this purpose, multiple strategies have been proposed to address the technical challenges in the POC area and field diagnosis based on optical/electrical components. For example, deep learning-based methods using the convolutional neural network architecture for SPR measurement precision enhancement are under development [117]. Another important aspect for marketing is related to the availability of low-cost plug-and-play devices for the diffusion of methods and technologies for the personalized monitoring of physiological parameters by wearable devices.

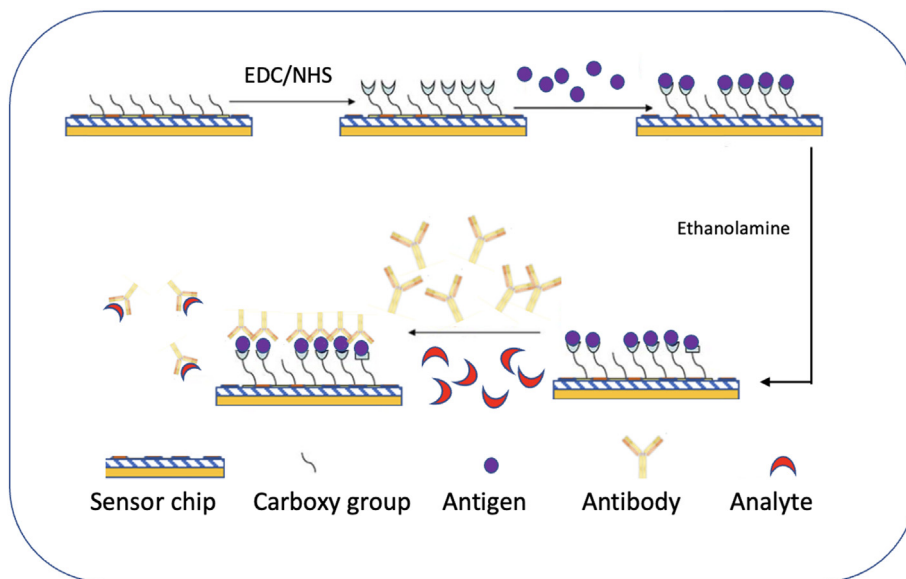


Fig. 13. Scheme of the SPR based competitive immunoassay for  $\text{Cd}^{2+}$ .

Cost-effective, portable, and rapid sensing systems play critical roles in bringing biodetection technologies from central laboratories to field application. Although laboratory-based benchtop instruments usually provide higher sensitivity and stability, they are usually expensive and bulky. For this reason, widespread low-cost and user-friendly external auxiliary tools, such as smartphones, are gradually standing out because of the global ubiquity, steady upgrading functions and straightforward coupling with optical methods that utilize absorbance/transmittance [118], chemiluminescence [119], spectroscopy of guided waves based on photonic crystal [120] and Surface Plasmon Resonance [121–123]. Unlike ELISA or PCR, SPR does not require a labeling procedure, which is a great advantage in field applications. Utilizing high-performance complementary metal–oxide–semiconductor (CMOS)-based cameras on smartphones, many groups have designed spectrum- and intensity-based SPR biosensors on

smartphone platforms. As examples, Guner et al. demonstrated a surface plasmon resonance imaging platform integrated with a smartphone to be used in the field with high-throughput biodetection [124]. In another work Zhang et al. applied a grating-coupled SPR smartphone spectrometer for the detection of lipopolysaccharides (LPS) [118], also known as endotoxins, present in drinking water and injectable biofluids that may trigger septic shock. In this work the authors described a portable LPS detection platform based on a smartphone and a grating-coupled SPR (GC-SPR) which relies on a disposable sensor chip with Au diffraction grating and a compact disk as the spectra dispersive unit. Although it does not contain electronic components, the use of apertures, polarizers, and diffraction gratings increases the complexity of the optical configuration. However, a limitation to their actual diagnostic usefulness is represented by the need to analyze the images captured by the smartphone on the computer. As the optical

Table 5  
Modern smartphone-based SPR sensors [137].

Principle	Smartphone utilization	Application/Detection	Performance Limit of Detection (LOD)	Ref.
LSPR	Camera and LED	Heart disease biomarker <i>Cardiac human troponin I</i>	50 ng/mL	[125]
	Camera	Protein <i>Bovine Serum Albumin (BSA)</i>	19.2 $\mu\text{g/mL}$	[126]
		Water pollutant $\text{NH}_3$	200 $\mu\text{g/mL}$	[127]
		Water pollutant $\text{Cr}^{3+}$	11 $\mu\text{M}$	[128]
		Water pollutant $\text{Hg}^{2+}$	0.2 ppb	[129]
		Water pollutant $\text{Cd}^{2+}$	1.12 ng/mL	[130]
		Cancer biomarker <i>CA13-5</i>	0.87 U/mL	[131]
Prism coupled	Camera and screen	Cancer marker <i>Microglobulin (2 M)</i>	0.1 $\mu\text{g/mL}$	[122]
	Camera	Antibiotic <i>Doxycycline</i>	$2.25 \times 10^{-11}$ $\mu\text{M}$	[132]
Waveguide coupled	Camera and LED	Antibody in blood <i>Immunoglobulin G (IgG)</i>	47.4 nM	[121]
Grating coupled	Camera and LED	Endotoxin <i>Lipopolysaccharides</i>	20 $\mu\text{g/mL}$	[133]
	Camera	Pesticide <i>Imidacloprid</i>	32.5 ng/mL	[118]
		Protein <i>Bovine Serum Albumin (BSA)</i>	1 ppb	[134]
		Protein <i>Bovine Serum Albumin (BSA)</i>	1 $\mu\text{g/mL}$	[135]
			2.43 $\mu\text{g/mL}$	[136]



intensity at fixed angle or wavelength is monitored by smartphones in real time, intensity-based assay is attracting much attention because of its low-cost, simplicity, and practicality, providing real-time data analysis and being usually stable, inexpensive, and simple to perform [133].

A list of modern smartphone-based SPR sensors and their applications of detection is provided in Table 5.

## 7. Conclusion

In this review, we discussed the recent advancements in the SPR technology along with application examples and on-market instrumentation descriptions. Despite the significant progress in many fields from the biotechnology sector, pharmaceutical industry, clinical research, and many others, Surface Plasmon Resonance technology suffers from two main shortcomings, high cost and complexity of use. For this reason, SPR technology still needs further improvements and its exploitation as a tool for routine analysis is a challenge that today seems realistic.

At this purpose, some smartphone-based SPR platforms have been already developed and could represent a low-cost and sensitive approach to the rapid detection of a variety of analytes, offering the advantage of carrying out on-site and remote detection of environmental and biomedical samples and use in point-of-care devices, as well as being a practical platform for household devices. Moreover, the continued progression of artificial intelligence, big data, 5G technology, wearable devices, and databases established through patient information and telemedicine services, generates important expectations.

## Declaration of competing interest

The authors declare that they have no known competing financial interests or personal relationships that could have appeared to influence the work reported in this paper.

## Data availability

No data was used for the research described in the article.

## References

- [1] M.A. Cooper, Optical biosensors in drug discovery, *Nat. Rev. Drug Discov.* 1 (2002) 515–528. <https://doi.org/10.1038/nrd838>. R.B.M. Schasfoort, History and Physics of Surface Plasmon Resonance, in: R.B.M. Schasfoort (Eds.), *Handbook of Surface Plasmon Resonance*, second ed., Royal Society of Chemistry, London, 2017. <https://doi.org/10.1039/9781788010283>.
- [2] R.L. Rich, D.G. Myszka, Advances in surface plasmon resonance biosensor analysis, *Curr. Opin. Biotechnol.* 11 (2000) 54–61. [https://doi.org/10.1016/S0958-1669\(99\)00054-3](https://doi.org/10.1016/S0958-1669(99)00054-3).
- [3] A. Eciya-Arenas, E.M. Kirchner, T. Hirscher, J.M. Fernandez-Romero, Development of an aptamer-based SPR-biosensor for the determination of kanamycin residues in foods, *Anal. Chim. Acta* 1169 (2021), 338631. <https://doi.org/10.1016/j.aca.2021.338631>.
- [4] W. Wang, Z. Mai, Y. Chen, J. Wang, L. Li, Q. Su, X. Li, X. Hong, A label-free fiber optic SPR biosensor for specific detection of C-reactive protein, *Sci. Rep.* 7 16904 (2017). <https://doi.org/10.1038/s41598-017-17276-3>.
- [5] L.L.S. Canabady-Rochelle, K. Selmezi, S. Collin, A. Pasc, L. Muhr, S. Boschi-Muller, SPR screening of metal chelating peptides in a hydrolysate for their antioxidant properties, *Food Chem.* 239 (2018) 478–485. <https://doi.org/10.1016/j.foodchem.2017.06.116>.
- [6] R. Pilolli, L. Monaci, Challenging the limit of detection for egg allergen detection in red wines by surface plasmon resonance biosensor, *Food Anal. Methods* 9 (2016) 2754–2761. <https://doi.org/10.1007/s12161-016-0464-z>.
- [7] J. Homola, Surface plasmon resonance sensors for detection of chemical and biological species, *Chem. Rev.* 108 (2008) 462–493. <https://doi.org/10.1021/cr068107d>.
- [8] C. Situ, M.H. Mooney, C.T. Elliott, J. Buijs, Advances in surface plasmon resonance biosensor technology towards high-throughput, food-safety analysis, *TrAC, Trends Anal. Chem.* 29 (2010) 1305–1315. <https://doi.org/10.1016/j.trac.2010.09.003>.
- [9] L. Gorton, Biosensors and modern biospecific analytical techniques, in: *Comprehensive Analytical Chimica*, Elsevier, Amsterdam, 2005. [https://doi.org/10.1016/s0166-526x\(05\)x4400-2](https://doi.org/10.1016/s0166-526x(05)x4400-2), 44.
- [10] D. Huddler, E.R. Zartler, *Applied Biophysics for Drug Discovery*, Wiley, Hoboken, 2017. <https://doi.org/10.1002/9781119099512>.
- [11] R.B.M. Schasfoort (Editor), *Handbook of Surface Plasmon Resonance*, second ed., Royal Society of Chemistry, London, 2017. <https://doi.org/10.1039/9781788010283>.
- [12] *Biacore Technology Handbook*, Pharmacia Biosensor AB, Uppsala, 1994.
- [13] J. Homola, Electromagnetic theory of surface plasmons, in: J. Homola, O.S. Wolfbeis (Editors), *Surface Plasmon Resonance Based Sensors*, Springer Series on Chemical Sensors and Biosensors, Springer, Berlin, Heidelberg, 2006, pp. 3–44. [https://doi.org/10.1007/5346\\_013](https://doi.org/10.1007/5346_013), 4.
- [14] R.B.M. Schasfoort, History and Physics of Surface Plasmon Resonance, in: R.B.M. Schasfoort (Editor), *Handbook of Surface Plasmon Resonance*, second ed., Royal Society of Chemistry, London, 2017. <https://doi.org/10.1039/9781788010283>.
- [15] Q. Wang, Z.H. Ren, W.M. Zhao, L. Wang, X. Yan, A.S. Zhu, F.M. Qiu, K.K. Zhang, Research advances on surface plasmon resonance biosensors, *Nanoscale* 14 (2022) 564–591. <https://doi.org/10.1039/D1NR05400G>.
- [16] A. Steinegger, O.S. Wolfbeis, S.M. Borisov, Optical sensing and imaging of pH values: spectroscopies, materials, and applications, *Chem. Rev.* 120 (2020) 12357–12489. <https://doi.org/10.1021/acs.chemrev.0c00451>.
- [17] M. Zekriti, Temperature effects on the resolution of surface-plasmon-resonance-based sensor, *Plasmonics* 14 (2019) 763–768. <https://doi.org/10.1007/s11468-018-0855-7>.
- [18] R.W. Wood, On a remarkable case of uneven distribution of light in a diffraction grating spectrum, *Proc. Phys. Soc.* 18 (1902) 269.
- [19] R.W. Wood, Diffraction gratings with controlled groove form and abnormal distribution of intensity, *Philos. Mag.* A 23 (1912) 310–317.
- [20] U. Fano, The theory of anomalous diffraction gratings and of quasi-stationary waves on metallic surfaces (Sommerfeld's waves), *J. Opt. Soc. Am.* 31 (1941) 213–222.
- [21] T. Thurbadar, Complete absorption of light by thin metal films, *Proc. Phys. Soc.* 73 (1959) 40.
- [22] A. Otto, Excitation of surface plasma waves in silver by the method of frustrated total reflection, *Z. Phys.* 216 (1968) 398–410. <https://doi.org/10.1007/BF01391532>.
- [23] E. Kretschmann, H. Raether, Notizen: radiative decay of non radiative surface plasmons excited by light, *Z. Naturforsch.* 23 (1968) 2135–2136. <https://doi.org/10.1515/zna-1968-1247>.
- [24] J. Homola, H.B. Lu, G.G. Nenninger, J. Dostalek, S.S. Yee, A novel multichannel surface plasmon resonance biosensor, *Sens. Actuators B Chem.* 76 (2001) 403–410. [https://doi.org/10.1016/S0925-4005\(01\)00648-7](https://doi.org/10.1016/S0925-4005(01)00648-7).
- [25] Y. Wei, Y. Su, C. Liu, X. Nie, Z. Liu, Y. Zhang, Y. Zhang, Two-Channel SPR sensor combined application of polymer- and vitreous-clad optic fibers, *Sensors* 17 (2017), 2862. <https://doi.org/10.3390/s17122862>.
- [26] L. Sarcina, E. Macchia, G. Loconsole, G. D'Attoma, P. Saldarelli, V. Elicio, G. Palazzo, L. Torsi, Surface plasmon resonance assay for label-free and selective detection of xylella fastidiosa, *Adv. Nanobiomed Res.* 1 (2021) 1–8. <https://doi.org/10.1002/anbr.202100043>.
- [27] R.B.M. Schasfoort, Surface Plasmon Resonance Instruments, in: R.B.M. Schasfoort (Editor), *Handbook of Surface Plasmon Resonance*, second ed., Royal Society of Chemistry, London, 2017. <https://doi.org/10.1039/9781788010283>.
- [28] Cytiva. <https://www.cytivalifesciences.com/en/us/shop/protein-analysis/spr-label-free-analysis/systems>, 2022. (Accessed 30 September 2022). accessed.
- [29] Bruker. <https://www.bruker.com/en/products-and-solutions/surface-plasmon-resonance.html>, 2022. (Accessed 30 September 2022). accessed.
- [30] J.A. Marquart, Surface plasmon resonance and biomolecular interaction analysis, in: *Theory and Practice*, fourth ed., 2013. Unknown publisher.
- [31] A.G. Sartorius. <https://www.sartorius.com/en/products/protein-analysis/onestep-spr-systems>, 2022. (Accessed 30 September 2022). accessed.
- [32] J.G. Quinn, Modeling Taylor dispersion injections: determination of kinetic/affinity interaction constants and diffusion coefficients in label-free biosensing, *Anal. Biochem.* 421 (2012) 391–400. <https://doi.org/10.1016/j.jab.2011.11.024>.
- [33] K. Narayan, S.S. Carroll, SPR Screening: Applying the New Generation of SPR Hardware, in: D. Huddler, E.R. Zartler (Editors), *Applied Biophysics for Drug Discovery*, Wiley, Hoboken, 2017. <https://doi.org/10.1002/9781119099512>.
- [34] L.E. Hartley-Tassell, M.M. Awad, K.L. Seib, M. Scarselli, S. Savino, J. Tiralongo, D. Lyras, C.J. Day, M.P. Jennings, Lectin activity of the TcdA and TcdB toxins of *Clostridium difficile*, *Infect. Immun.* 87 (2019). <https://doi.org/10.1128/IAI.00676-18>.
- [35] Marvel Panalytical Ltd. <https://www.marvernpanalytical.com/en/products/product-range/WAVE/>, 2022. (Accessed 30 September 2022). accessed.
- [36] XanTech bioanalytics GmbH. <https://www.xantec.com/products/spr-biosensors/sprplus.php>, 2022. (Accessed 30 September 2022). accessed.
- [37] ReichterInc. <https://www.reichterspr.com/spr-systems/reichert-spr-systems>, 2022. (Accessed 30 September 2022). accessed.
- [38] FOX Biosystems. <https://foxbiosystems.com/white-fox-biosensing-technology-fox-biosystems/>, 2022. (Accessed 30 September 2022). accessed.
- [39] Affinité Instruments. <https://www.affiniteinstruments.com/>, 2022. (Accessed 30 September 2022). accessed.
- [40] PhotonicSys Ltd. <https://www.photonicsys.com/products-1>, 2022. (Accessed 30 September 2022). accessed.

- [41] Plasmetrix. <https://plasmetrix.com/>, 2022. (Accessed 30 September 2022). accessed.
- [42] E.T. Gedig, Surface chemistry in SPR technology, in: R.B.M. Schasfoort (Editor), *Handbook of Surface Plasmon Resonance*, second ed., Royal Society of Chemistry, London, 2017. <https://doi.org/10.1039/9781788010283>.
- [43] A.G. Brolo, Plasmonic for future biosensors, *Nat. Photonics* 6 (2012) 709–713. <https://doi.org/10.1038/nphoton.2012.266>.
- [44] M. Piliarik, H. Vaisocherová, J. Homola, Surface plasmon resonance biosensing, in: A. Rasooly, K.E. Herold (Editors), *Biosensors and Biodection. Methods in Molecular Biology*, Humana Press, Totowa, 2009, pp. 65–88. [https://doi.org/10.1007/978-1-60327-567-5\\_5](https://doi.org/10.1007/978-1-60327-567-5_5), 503.
- [45] H.H. Nguyen, J. Park, S. Kang, M. Kim, Surface plasmon resonance: a versatile technique for biosensor applications, *Sensors* 15 (2015) 10481–10510. <https://doi.org/10.3390/s150510481>.
- [46] N. Ravindran, S. Kumar, M. Yashini, S. Rajashwari, C.A. Mamathi, S.N. Thirunavookarasu, C.K. Sunil, Recent adv. Surf. Plasmon Reson. (SPR) biosens. food anal.: a review, *Crit. Rev. Food Sci. Nutr* (2021) 1–23. <https://doi.org/10.1080/10408398.2021.1958745>.
- [47] B.A. Sexton, B.N. Feltis, T.J. Davis, Characterisation of gold surface plasmon resonance sensor substrates, *Sens. Actuators A Phys.* 141 (2008) 471–475. <https://doi.org/10.1016/j.sna.2007.10.020>.
- [48] *Biacore™, Sensor Surface Handbook*, Cytiva, 2022.
- [49] G.V. Naik, V.M. Shalae, A. Boltasheva, Alternative plasmonic materials: beyond gold and silver, *Adv. Mater.* 25 (2013) 3264–3294. <https://doi.org/10.1002/adma.201205076>.
- [50] G. Wang, C. Wang, R. Yang, W. Liu, S. Sun, A. Sensitive, Stable Surface, Plasmon resonance sensor based on monolayer protected silver film, *sensors*, 17 2777 (2017). <https://doi.org/10.3390/s17122777>.
- [51] G. Wang, L. Huang, Sensitivity enhancement of a silver based surface plasmon resonance sensor via an optimizing graphene-dielectric composite structure, *Appl. Opt.* 61 (2022) 683–690. <https://doi.org/10.1364/AO.446579>.
- [52] E.P. Rodrigues, L.C. Oliveira, M.L.F. Silva, C.S. Moreira, A.M.N. Lima, Surface plasmon resonance sensing characteristics of thin copper and gold films in aqueous and gaseous interfaces, *IEEE, Sens. J.* 20 (2020) 7701–7710. <https://doi.org/10.1109/JSEN.2020.2980388>.
- [53] N. Beydoun, Y. Niberon, L. Arnaud, J. Proust, K. Nomenyo, S. Zeng, G. Lerondel, A. Bruyant, Stabilization of copper-based biochips with alumina for biosensing application, *Biosensors* 12 (2022), 1132. <https://doi.org/10.3390/bios12121132>.
- [54] R.B.M. Schasfoort, Introduction to Surface Plasmon Resonance, in: R.B.M. Schasfoort (Editor), *Handbook of Surface Plasmon Resonance*, second ed., Royal Society of Chemistry, London, 2017. <https://doi.org/10.1039/9781788010283>.
- [55] *Biacore Sensor Surface Handbook BR-1005-71*, GE Healthcare Bio-Sciences AB, Uppsala, in: AB (Editor), 2005.
- [56] S. Mariani, M. Minunni, Surface plasmon resonance applications in clinical analysis, *Anal. Bioanal. Chem.* 406 (2014) 2303–2323. <https://doi.org/10.1007/s00216-014-7647-5>.
- [57] S. Lofas, B. Johnsson, A. Edstrom, A. Hansson, G. Lindquist, R.M. Muller Hillgren, L. Stigh, Methods for site controlled coupling to carboxymethyl dextran surfaces in surface plasmon resonance sensors, *Biosens. Bioelectron.* 10 (1995) 813–822. [https://doi.org/10.1016/0956-5663\(95\)99220-F](https://doi.org/10.1016/0956-5663(95)99220-F).
- [58] K. Kambhampati, T.A.M. Jakob, J.W. Robertson, M. Cai, J.E. Pemberton, W. Knoll, *Langmuir* 17 (2001) 1169–1175. <https://doi.org/10.1021/la001250w>.
- [59] M.R. Lockett, S.C. Weibel, M.F. Phillips, M.R. Shortreed, B. Sun, R.M. Corn, R.J. Hamers, F. Cerrina, L.M. Smith, Carbon-on-metal films for surface plasmon resonance detection of DNA arrays, *J. Am. Chem. Soc.* 130 (2008) 8611–8613. <https://doi.org/10.1021/ja802454c>.
- [60] L. Wu, H.S. Chu, W.S. Koh, E.P. Li, Highly sensitive graphene biosensors based on surface plasmon resonance, *Opt Express* 18 (2010) 14395–14400. <https://doi.org/10.1364/OE.18.014395>.
- [61] B.D. Lang, M. Delmar, W. Coombs, Surface Plasmon Resonance as a Method to Study the Kinetics and Amplitude of Protein-Protein Binding, in: S. Dhein, F.W. Mohr, M. Delmar (Editors), *Practical Methods in Cardiovascular Research*, Springer, Berlin, Heidelberg, 2005, pp. 936–947. [https://doi.org/10.1007/3-540-26574-0\\_47](https://doi.org/10.1007/3-540-26574-0_47).
- [62] S. Lofas, A. McWhirter, The art of immobilization for SPR sensors, in: J. Homola, O.S. Wolfbeis (Editors), *Surface Plasmon Resonance Based Sensors. Springer Series on Chemical Sensors and Biosensors*, Springer, Berlin, Heidelberg, 2006, pp. 117–151. [https://doi.org/10.1007/5346\\_013](https://doi.org/10.1007/5346_013), 4.
- [63] M.J.E. Fischer, Amine coupling through EDC/NHS: a practical approach, in: N.J. de Mol, M.J.E. Fischer (Editors), *Surface Plasmon Resonance: Methods and Protocols*, Humana Press, Totowa, 2010.
- [64] A.A. Kortt, G.W. Oddie, P. Iliades, L.C. Gruen, P.J. Hudson, Nonspecific amine immobilization of ligand can be a potential source of error in BiAcCore binding experiments and may reduce binding affinities, *Anal. Biochem.* 253 (1997) 103–111. <https://doi.org/10.1006/abio.1997.2333>.
- [65] G.T. Hermanson, in: *Bioconjugate Techniques, third ed.*, Academic Press, Cambridge, 2013.
- [66] J.V. Staros, R.W. Wright, D.M. Swingle, Enhancement by N-hydroxysulfosuccinimide of water-soluble carbodiimide-mediated coupling reactions, *Anal. Biochem.* 156 (1986) 220–222. [https://doi.org/10.1016/0003-2697\(86\)90176-4](https://doi.org/10.1016/0003-2697(86)90176-4).
- [67] J.L. Lichty, J.L. Malecki, H.D. Agnew, D.J. Michelson-Horowitz, S. Tan, Comparison of affinity tags for protein purification, *Protein Expr, Purif* 41 (2005) 98–105. <https://doi.org/10.1016/j.jep.2005.01.019>.
- [68] S.Q. Hutsell, R.J. Kimple, D.P. Siderovski, F.S. Willard, A.J. Kimple, High-affinity immobilization of proteins using biotin- and GST-based coupling strategies, *Methods Mol. Biol.* 627 (2010) 75–90. [https://doi.org/10.1007/978-1-60761-670-2\\_4](https://doi.org/10.1007/978-1-60761-670-2_4).
- [69] P.R. Edwards, A. Gill, D.V. Pollard-Knight, M. Hoare, P.E. Buckle, P.A. Lowe, R.J. Leatherbarrow, Kinetics of protein-protein interactions at the surface of an optical biosensor, *Anal. Biochem.* 231 (1995) 210–217. <https://doi.org/10.1006/abio.1995.1522>.
- [70] R.W. Glaser, Antigen-antibody binding and mass transport by convection and diffusion to a surface: a two-dimensional computer model of binding and dissociation kinetics, *Anal. Biochem.* 213 (1993) 152–161. <https://doi.org/10.1006/abio.1993.1399>.
- [71] D.G. Myszkka, X. He, M. Dembo, T.A. Morton, B. Goldstein, Extending the range of rate constants available from BIACORE: interpreting mass transport-influenced binding data, *Biophys. J.* 75 (1998) 583–594. [https://doi.org/10.1016/S0006-3495\(98\)77549-6](https://doi.org/10.1016/S0006-3495(98)77549-6).
- [72] D.G. Myszkka, T.A. Morton, M.L. Doyle, I.M. Chaiken, Kinetic analysis of a protein antigen-antibody interaction limited by mass transport on an optical biosensor, *Biophys. Chem.* 64 (1997) 127–137. [https://doi.org/10.1016/S0301-4622\(96\)02230-2](https://doi.org/10.1016/S0301-4622(96)02230-2).
- [73] AA (Editor), *Biacore Assay Handbook 29-0194-00*, GE Healthcare Bio-Sciences AB, Uppsala, 2012.
- [74] K. Andersson, D. Areskou, E. Hardenborg, Exploring buffer space for molecular interactions, *J. Mol. Recogn.* 12 (1999) 310–315. [https://doi.org/10.1002/\(SICI\)1099-1352\(199909/10\)12:5<310::AID-JMR470>3.0.CO;2-5](https://doi.org/10.1002/(SICI)1099-1352(199909/10)12:5<310::AID-JMR470>3.0.CO;2-5).
- [75] R.J. Ober, E.S. Ward, The choice of reference cell in the analysis of kinetic data using BiAcCore, *anal. Biochem* 271 (1999) 70–80. <https://doi.org/10.1006/abio.1999.4129>.
- [76] A. Frostell-Karlsson, A. Remaeus, H. Roos, K. Andersson, P. Borg, M. Hamalainen, R. Karlsson, Biosensor analysis of the interaction between immobilized human serum albumin and drug compounds for prediction of human serum albumin binding levels, *J. Med. Chem.* 43 (2000) 1986–1992. <https://doi.org/10.1021/jm991174y>.
- [77] D.G. Myszkka, Improving biosensor analysis, *J. Mol. Recogn.* 12 (1999) 279–284. [https://doi.org/10.1002/\(SICI\)1099-1352\(199909/10\)12:5<279::AID-JMR473>3.0.CO;2-3](https://doi.org/10.1002/(SICI)1099-1352(199909/10)12:5<279::AID-JMR473>3.0.CO;2-3).
- [78] D.G. Myszkka, T.A. Morton, CLAMP: a biosensor kinetic data analysis program, *Trends Biochem. Sci.* 23 (1998) 149–150. [https://doi.org/10.1016/S0968-0004\(98\)01183-9](https://doi.org/10.1016/S0968-0004(98)01183-9).
- [79] G.A. Navratilova, R.L. Papalia, D. Rich, S. Bedinger, B. Brophy, T. Condon, A.W. Deng, H.W. Emerick, T. Guan, T. Hayden, B. Heutmekers, M.C. Hoorelbeke, M.M. McCroskey, T. Murphy, F. Nakagawa, X. Parmeggiani, S. Qin, N. Rebe, T. Tomasevic, M.B. Tsang, F.F. Waddell, S. Zhang, D.G. Leavitt, Myszkka, Thermodynamic benchmark study using BiAcCore technology, *Anal. Biochem.* 364 (2007) 67–77. <https://doi.org/10.1016/j.ab.2007.01.031>.
- [80] N.T. Ditto, J. Eckman, Treating raw data: software for SPR applications, in: R.B.M. Schasfoort (Editor), *Handbook of Surface Plasmon Resonance*, second ed., Royal Society of Chemistry, London, 2017. <https://doi.org/10.1039/9781788010283>.
- [81] SPRpages. <https://www.sprpages.nl/spr-software>, 2022. (Accessed 5 October 2022). accessed.
- [82] G. Dahl, S. Steigle, P. Hillertz, A. Tigerstrom, A. Egneus, A. Mehrle, M. Ginkel, F. Edfeldt, G. Holdgate, N. O'Connell, B. Kappler, A. Brodte, P.B. Rawlins, G. Davies, E.L. Westberg, R.H.A. Folmer, S. Heyse, Unified software solution for efficient SPR data analysis in drug research, *SLAS Discov* 22 (2017) 203–209. <https://doi.org/10.1177/1087057116675316>.
- [83] M. Lehrke, M.A. Lazar, The many faces of PPARgamma, *Cell* 123 (2005) 993–999. <https://doi.org/10.1016/j.cell.2005.11.026>.
- [84] P. Tontonoz, B.M. Spiegelman, Fat and beyond: the diverse biology of PPARγ, *Annu. Rev. Biochem.* 77 (2008) 289–312. <https://doi.org/10.1146/annurev.biochem.77.061307.091829>.
- [85] R. Montanari, D. Capelli, A. Tava, A. Galli, A. Laghezza, P. Tortorella, F. Loidice, G. Pochetti, Screening of saponins and saponinins from *Medicago* species as potential PPARγ agonists and X-ray structure of the complex PPARγ/caulophylligenin, *Sci. Rep.* 6 (2016) 27658. <https://doi.org/10.1038/srep27658>.
- [86] R. Montanari, F. Saccoccia, E. Scotti, M. Crestani, C. Godio, F. Gilardi, F. Loidice, G. Fracchiolla, A. Laghezza, P. Tortorella, A. Lavecchia, E. Novellino, F. Mazza, M. Aschi, G. Pochetti, crystal structure of the peroxisome proliferator-activated receptor γ (PPARγ) ligand binding domain complexed with a novel partial agonist: a new region of the hydrophobic pocket could be exploited for drug design, *J. Med. Chem.* 51 (2008) 7768–7776. <https://doi.org/10.1021/jm800733h>.
- [87] R.L. Rich, L.R. Hoth, K.F. Geoghegan, D.G. Myszkka, Kinetic analysis of estrogen receptor/ligand interactions, *Proc. Natl. Acad. Sci. USA* 99 (2002) 8562–8567. <https://doi.org/10.1073/pnas.142288199>.
- [88] D. Capelli, C. Parravicini, G. Pochetti, R. Montanari, C. Temporini, M. Rabuffetti, M.L. Trincavelli, S. Daniele, M. Fumagalli, S. Saporiti, E. Bonfanti, M.P. Abbraccio, I. Eberini, S. Ceruti, E. Calleri, S. Capaldi, Surface plasmon resonance as a tool for ligand binding investigation of engineered GPR17 receptor, a G protein coupled receptor involved in myelination, *Front. Chem.* 7 (2020) 910. <https://doi.org/10.3389/fchem.2019.00910>.

- [89] R.L. Rich, J. Errey, F. Marshall, D.G. Myszk, Biacore analysis with stabilized G-protein-coupled receptors, *Anal. Biochem.* 409 (2011) 267–272. <https://doi.org/10.1016/j.ab.2010.10.008>.
- [90] J.A. Maynard, N.C. Lindquist, J.N. Sutherland, A. Lesuffleur, A.E. Warrington, M. Rodriguez, S.H. Oh, Surface plasmon resonance for high-throughput ligand screening of membrane-bound proteins, *Biotechnol. J.* 4 (2009) 1542–1558. <https://doi.org/10.1002/biot.200900195>.
- [91] S.G. Patching, Surface plasmon resonance spectroscopy for characterisation of membrane protein-ligand interactions and its potential for drug discovery, *Biochim. Biophys. Acta* 1838 (2014) 43–55. <https://doi.org/10.1016/j.bbame.2013.04.028>.
- [92] S. Locatelli-Hoops, A.A. Yeliseev, K. Gawrisch, I. Gorshkova, Surface Plasmon Resonance applied to G protein-coupled receptors, *Biomed. Spectrosc. Imag.* 2 (2013) 155–181. <https://doi.org/10.3233/BSI-130045>.
- [93] Lundquist, S.B. Hansen, H. Nordström, U.H. Danielson, K. Edwards, Biotinylated lipid bilayer disks as model membranes for biosensor analyses, *Anal. Biochem.* 405 (2010) 153–159. <https://doi.org/10.1016/j.ab.2010.06.030>.
- [94] M.P. Abbraccio, G. Burnstock, J.M. Boeynaems, E.A. Barnard, J.L. Boyer, C. Kennedy, G.E. Knight, M. Fumagalli, C. Gachet, K.A. Jacobson, G.A. Weisman, International union of pharmacology LVIII: update on the P2Y G protein-coupled nucleotide receptor: from molecular mechanism and pathophysiology to therapy, *Pharmacol. Rev.* 58 (2006) 281–341. <https://doi.org/10.1124/pr.58.3.3>.
- [95] P. Ciana, M. Fumagalli, M.L. Trincavelli, C. Verderio, P. Rosa, D. Lecca, S. Ferrario, C. Parravicini, V. Capra, P. Gelosa, U. Guerrini, S. Belcredito, M. Cimino, L. Sironi, E. Tremoli, G.E. Trovati, C. Martini, M.P. Abbraccio, The orphan receptor GPR17 identified as a new dual uracil nucleotides/cysteinyll-leukotrienes receptor., *EMBO J.* 25 (2006) 4615–4627. <https://doi.org/10.1038/sj.emboj.7601341>.
- [96] I. Eberini, S. Daniele, C. Parravicini, C. Sensi, M.L. Trincavelli, C. Martini, M.P. Abbraccio, In silico identification of new ligands for GPR17: a promising therapeutic target for neurodegenerative diseases, *J. Comput. Aided Mol. Des.* 25 (2011) 743–752. <https://doi.org/10.1007/s10822-011-9455-8>.
- [97] R. Montanari, D. Capelli, K. Yamamoto, H. Awaishima, K. Nishikata, A. Berendregt, A.J.R. Heck, F. Loidice, F. Altieri, A. Paiardini, A. Grottesi, L. Pirone, E. Pedone, F. Peiretti, J.M. Brunel, T. Itoh, G. Pochetti, Insights into PPAR $\gamma$  phosphorylation and its inhibition mechanism, *J. Med. Chem.* 63 (2020) 4811–4823. <https://doi.org/10.1021/acs.jmedchem.0c00048>.
- [98] J.H. Choi, A.S. Banks, J.L. Estall, S. Kajimura, P. Bostrom, D. Laznik, J.L. Ruas, M.J. Chalmers, T.M. Kamenecka, M. Blucher, P.R. Griffin, B.M. Spiegelman, Anti-diabetic drugs inhibit obesity-linked phosphorylation of PPARgamma by Cdk5, *Nature* 466 (2010) 451–456. <https://doi.org/10.1038/nature09291>.
- [99] A. Laghezza, L. Piemontese, C. Cerchia, Montanari, D. Capelli, M. Giudici, M. Crestani, P. Tortorella, F. Peiretti, G. Pochetti, A. Lavecchia, F. Loidice, identification of the first PPARalpha/gamma dual agonist able to bind to canonical and alternative sites of PPARgamma and to inhibit its cdk5-mediated phosphorylation, *J. Med. Chem.* 61 (2018) 8282–8298. <https://doi.org/10.1021/acs.jmedchem.8b00835>.
- [100] J.Y. Jang, M. Koh, H. Bae, D.R. An, H.N. Im, H.S. Kim, J.Y. Yoon, H.J. Yoon, B.W. Han, S.B. Park, S.W. Suh, Structural basis for differential activities of enantiomeric PPARgamma agonists: binding of S35 to the alternate site, *Biochim. Biophys. Acta, Proteins Proteomics* 1865 (2017) 674–681. <https://doi.org/10.1016/j.bbapap.2017.03.008>.
- [101] R. Brust, H. Lin, J. Fuhrmann, A. Asteian, T.M. Kamenecka, D.J. Kojetin, Modification of the orthosteric PPARgamma covalent antagonist scaffold yields an improved dual-site allosteric inhibitor, *ACS Chem. Biol.* 12 (2017) 969–978. <https://doi.org/10.1021/acschembio.6b01015>.
- [102] S. Spizzichino, D. Boi, G. Boumisi, R. Lucchi, F.R. Liberati, D. Capelli, R. Montanari, G. Pochetti, R. Piacentini, G. Parisi, A. Paone, S. Rinaldo, R. Contestabile, A. Tramonti, A. Paiardini, G. Giardina, F. Cutruzzola, Cytosolic localization and *in vitro* assembly of human *de novo* thymidylate synthesis complex, *FEBS J.* 289 (2022) 1625–1649. <https://doi.org/10.1111/febs.16248>.
- [103] T. Vorup-Jensen, On the roles of polyvalent binding in immune recognition: perspectives in the nanoscience of immunology and the immune response to nanomedicines, *Adv. Drug Deliv. Rev.* 64 (2012) 1759–1781. <https://doi.org/10.1016/j.addr.2012.06.003>.
- [104] A. Jendroszek, M. Kjaergaard, Nanoscale spatial dependence of avidity in an IgG1 antibody, *Sci. Rep.* 11 12663 (2021). <https://doi.org/10.1038/s41598-021-92280-2>.
- [105] R. Du, C. Huang, K. Liu, X. Li, Z. Dong, Targeting AURKA in Cancer: molecular mechanisms and opportunities for Cancer therapy, *Mol. Cancer* 20 (2021) 1–27. <https://doi.org/10.1186/s12943-020-01305-3>.
- [106] J.I. Johnsen, C. Dyberg, M. Wickstrom, Neuroblastoma—a neural crest derived embryonal malignancy, *Front. Mol. Neurosci.* 12 (2019) 1–11. <https://doi.org/10.3389/fnmol.2019.00009>.
- [107] T. Otto, S. Horn, M. Brockmann, U. Eilers, L. Schuttrumpf, N. Popov, A.M. Kenney, J.H. Schulte, R. Beijersbergen, H. Christiansen, B. Berwanger, M. Eilers, Stabilization of N-Myc is a critical function of Aurora A in human neuroblastoma, *Cancer Cell* 15 (2009) 67–78. <https://doi.org/10.1016/j.ccr.2008.12.005>.
- [108] G. Buchel, A. Carstensen, K.Y. Mak, I. Roeschert, E. Leen, O. Sumara, J. Hofstetter, S. Herold, J. Kalb, A. Baluapuri, E. Poon, C. Kwok, L. Chesler, H.M. Maric, D.S. Rickman, E. Wolf, R. Bayliss, S. Walz, M. Eilers, Association with aurora-A controls N-MYC-Dependent promoter escape and pause release of RNA polymerase II during the cell cycle, *Cell Rep.* 21 (2017) 3483–3497. <https://doi.org/10.1016/j.celrep.2017.11.090>.
- [109] D. Boi, F. Souvalidou, D. Capelli, F. Polverino, G. Marini, R. Montanari, G. Pochetti, A. Tramonti, R. Contestabile, D. Trisciuoglio, P. Carpinelli, C. Ascaneli, C. Lindon, A. De Leo, M. Saviano, R. Di Santo, R. Costi, G. Guarguaglini, A. Paiardini, PHA-680626 is an effective inhibitor of the interaction between aurora-A and N-myc, *int. J. Mol. Sci.* 22 13122 (2021). <https://doi.org/10.3390/ijms222313122>.
- [110] J. Gasparik, D. Vadarova, M. Capcarova, P. Smehyl, J. Slamecka, P. Garaj, R. Stawarz, P. Massanyi, Concentration of lead, cadmium, mercury and arsenic in leg skeletal muscles of three species of wild birds, *J. Environ. Sci. Health, Part A: Toxic/Hazard. Subst. Environ. Eng.* 45 (2010) 818–823. <https://doi.org/10.1080/10934521003708992>.
- [111] C. Cloquet, J. Carignan, G. Libourel, T. Sterckeman, E. Perdrix, Tracing source pollution in soils using cadmium and lead isotopes, *Environ. Sci. Technol.* 40 (2006) 2525–2530. <https://doi.org/10.1021/es052232+>.
- [112] Y. Cai, Y.J. Zhang, D.F. Wu, Y.L. Yu, J.H. Wang, Nonthermal optical emission spectrometry: direct atomization and excitation of cadmium for highly sensitive determination, *Anal. Chem.* 88 (2016) 4192–4195. <https://doi.org/10.1021/acs.analchem.6b00830>.
- [113] Y.J. Zhang, Y. Cai, Y.L. Yu, J.H. Wang, A miniature optical emission spectrometric system in a lab-on-valve for sensitive determination of cadmium, *Anal. Chim. Acta* 976 (2017) 45–51. <https://doi.org/10.1016/j.aca.2017.04.055>.
- [114] G.F. Cang, Y.Z. Yang, Y.F. Bai, Z.Z. Chenb, F. Feng, Surface Plasmon Resonance based competitive immunoassay for the detection of cadmium (Cd<sup>2+</sup>) in water samples, *RSC Adv.* 7 (2017) 44054–44058. <https://doi.org/10.1039/C7RA07635E>.
- [115] L. Monaci, I. Losito, F. Palmisano, A. Visconti, Identification of allergenic milk proteins markers in fined white wines by capillary liquid chromatography-electrospray ionization-tandem mass spectrometry, *J. Chromatography A* 1217 (2010) 4300–4305. <https://doi.org/10.1016/j.chroma.2010.04.035>.
- [116] D. Lebesi, C. Dimakou, A.J. Alldrick, V. Oreopoulou, Rapid test methods: a versatile tool to assist food-safety management, *Qual. Assur. Saf. 2* (2010) 173–181. <https://doi.org/10.1111/j.1757-837X.2010.00080.x>.
- [117] K. Thadson, S. Sasivimolkul, P. Suvarnapaht, S. Visitsattapongse, S. Pechprasarn, Measurement precision enhancement of surface plasmon resonance based angular scanning detection using deep learning, *Sci. Rep.* 12 2052 (2022). <https://doi.org/10.1038/s41598-022-06065-2>.
- [118] J. Zhang, I. Khan, Q. Zhang, X. Liu, J. Dostalek, B. Liedberg, Y. Wang, Lipopolysaccharides detection on a grating-coupled surface plasmon resonance smartphone biosensor, *Biosens. Bioelectron.* 99 (2018) 312–317. <https://doi.org/10.1016/j.bios.2017.07.048>.
- [119] M. Zangheri, L. Cevenini, L. Anfossi, C. Baggiani, P. Simoni, F. Di Nardo, A. Roda, A simple and compact smartphone accessory for quantitative chemiluminescence-based lateral flow immunoassay for salivary cortisol detection, *Biosens. Bioelectron.* 64 (2015) 63–68. <https://doi.org/10.1016/j.bios.2014.08.048>.
- [120] D. Gallegos, K.D. Long, H. Yu, P.P. Clark, Y. Lin, S. George, P. Nath, B.T. Cunningham, Label-free biodetection using a smartphone, *Lab Chip*, 13 2124 (2013). <https://doi.org/10.1039/C3LC40991K>.
- [121] Y. Liu, Q. Liu, S. Chen, F. Cheng, H. Wang, W. Peng, Surface plasmon resonance biosensor based on smart phone platforms, *sci. Rep.* 5 12864 (2015). <https://doi.org/10.1038/srep12864>.
- [122] P. Preechaburana, M. Collado Gonzalez, A. Suska, D. Filippini, Surface plasmon resonance chemical sensing on cell phones, *Angew. Chem. Int.* 51 (2012) 11585–11588. <https://doi.org/10.1002/anie.201206804>.
- [123] H. Wang, X. Wang, J. Wang, W. Fu, C. Yao, A SPR biosensor based on signal amplification using antibody-QD conjugates for quantitative determination of multiple tumor markers, *Sci. Rep.* 6 33140 (2016). <https://doi.org/10.1038/srep33140>.
- [124] H. Guner, E. Ozgur, G. Kokturk, M. Celik, E. Esen, A.E. Topal, S. Ayas, Y. Uludag, C. Elbuken, A. Dana, A smartphone based surface plasmon resonance imaging (SPRI) platform for on-site biodetection, *Sens. Actuators B Chem.* 239 (2017) 571–577. <https://doi.org/10.1016/j.snb.2016.08.061>.
- [125] Y. Wang, X. Liu, P. Chen, N.T. Tran, J. Zhang, W.S. Chia, S. Boujday, B. Liedberg, Smartphone spectrometer for colorimetric biosensing, *Analyst* 141 (2016) 3233–3238. <https://doi.org/10.1039/c5an02508g>.
- [126] S. Dutta, K. Saikia, P. Nath, Smartphone based LSPR sensing platform for bio-conjugation detection and quantification, *RSC Adv.* 6 (2016) 21871–21880. <https://doi.org/10.1039/c6ra01113f>.
- [127] A. Amirjani, D.H. Fatmehsari, Colorimetric detection of ammonia using smartphones based on localized surface plasmon resonance of silver nanoparticles, *Talanta* 176 (2018) 242–246. <https://doi.org/10.1016/j.talanta.2017.08.022>.
- [128] Y. Upadhyay, S. Bothra, R. Kumar, S.K. Sahoo, Smartphone-assisted colorimetric detection of Cr<sup>3+</sup> using Vitamin B6 cofactor functionalized gold nanoparticles and its applications in real sample analyses, *ChemistrySelect* 3 (2018) 6892–6896. <https://doi.org/10.1002/slct.201801289>.
- [129] S. Sajed, F. Arefi, M. Kolahdouz, M.A. Sadeghi, Improving sensitivity of mercury detection using learning based smartphone colorimetry, *Sensors Actuators B Chem.* 298 126942 (2019). <https://doi.org/10.1016/j.snb.2019.126942>.
- [130] Y. Gan, T. Liang, Q. Hu, L. Zhong, X. Wang, H. Wan, P. Wang, In-situ detection of cadmium with aptamer functionalized gold nanoparticles based on

- smartphone-based colorimetric system, *Talanta* 208 (2020), 120231. <https://doi.org/10.1016/j.talanta.2019.120231>.
- [131] Z. Fan, Z. Geng, W. Fang, X. Lv, Y. Su, S. Wang, H. Chen, Smartphone biosensor system with multi-testing unit based on localized surface plasmon resonance integrated with microfluidics chip, *Sensors* 20 (2020) 446. <https://doi.org/10.3390/s20020446>.
- [132] P.K. Badiya, S.S. Ramamurthy, Smartphone plasmonics for doxycycline detection with silver-lignin bio-spacer at attomolar sensitivity, *Plasmonics* 13 (2018) 955–960. <https://doi.org/10.1007/s11468-017-0593-2>.
- [133] Q. Liu, H. Yuan, Y. Liu, J. Wang, Z. Jing, W. Peng, Real-time biodetection using a smartphone-based dual-color surface plasmon resonance sensor, *J. Biomed. Opt.* 23 (2018) 1–6. <https://doi.org/10.1117/1.JBO.23.4.047003>.
- [134] K.L. Lee, M.L. You, C.H. Tsai, E.H. Lin, S.Y. Hsieh, M.H. Ho, J.C. Hsu, P.K. Wei, Nanoplasmonic biochips for rapid label-free detection of imidacloprid pesticides with a smartphone, *Biosens. Bioelectron.* 75 (2016) 88–95. <https://doi.org/10.1016/j.bios.2015.08.010>.
- [135] X. Wang, T. Chang, G. Lin, M.R. Gartia, G.L. Liu, Self-referenced smartphone-based nanoplasmonic imaging platform for colorimetric biochemical sensing, *Anal. Chem.* 89 (2017) 611–615. <https://doi.org/10.1021/acs.analchem.6b02484>.
- [136] M.Y. Pan, K.L. Lee, S.C. Lo, P.K. Wei, Resonant position tracking method for smartphone-based surface plasmon sensor, *Anal. Chim. Acta* 1032 (2018) 99–106. <https://doi.org/10.1016/j.aca.2018.05.033>.
- [137] G.P. Singh, N. Sardana, Smartphone-based Surface Plasmon Resonance Sensors: a Rev. *Plasm.* (2022) 1–20. <https://doi.org/10.1007/s11468-022-01672-1>.